CK2β Regulates Hematopoietic Stem Cell Biology and Erythropoiesis

Laura Quotti Tubi, Sara Canovas Nunes, Elisa Mandato, Marco Pizzi, Nicola Vitulo, Mirco D'agnolo, Raffaella Colombatti, Maddalena Martella, Maria Paola Boaro, Elena Doriguzzi Breatta, et al.

HemaSphere

EHA EUROPEAN HEMATOLOGY ASSOCIATION

Article
Open Access

CK2β Regulates Hematopoietic Stem Cell Biology and Erythropoiesis

Laura Quotti Tubi[1,2], Sara Canovas Nunes[2,3], Elisa Mandato[2,4], Marco Pizzi[5], Nicola Vitulo[6], Mirco D'Agnolo[7], Raffaella Colombatti[7], Maddalena Martella[7], Maria Paola Boaro[7], Elena Doriguzzi Breatta[1,2], Anna Fregnani[1,2], Zaira Spinello[1,2], Mitja Nabergoj[8], Odile Filhol[9], Brigitte Boldyreff[10], Mattia Albiero[11,12], Gian Paolo Fadini[12,13], Carmela Gurrieri[1,2], Fabrizio Vianello[1,2], Gianpietro Semenzato[1,2], Sabrina Manni[1,2], Livio Trentin[1,2], Francesco Piazza[1,2]

GRAPHICAL ABSTRACT

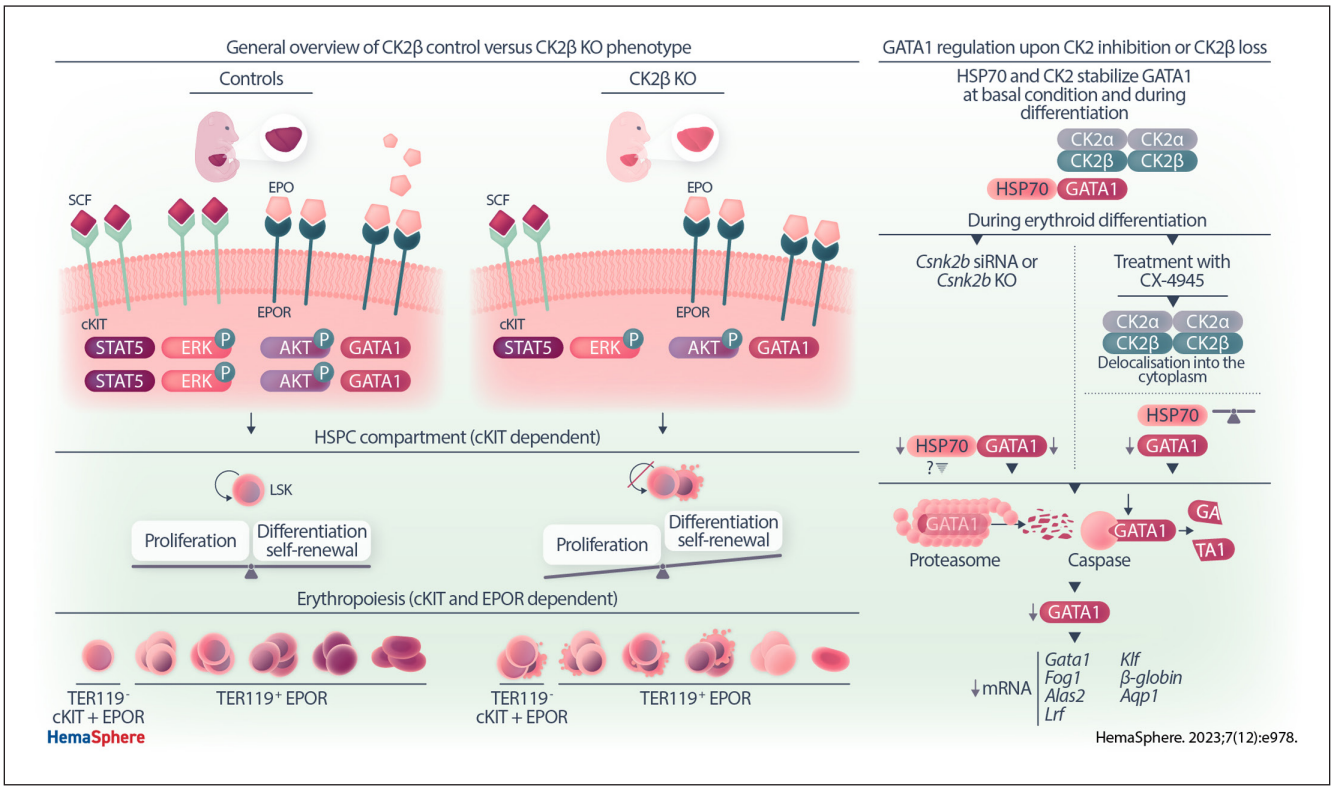

HemaSphere

EHA EUROPEAN HEMATOLOGY ASSOCIATION

Article
Open Access

CK2β Regulates Hematopoietic Stem Cell Biology and Erythropoiesis

Laura Quotti Tubi[1,2], Sara Canovas Nunes[2,3], Elisa Mandato[2,4], Marco Pizzi[5], Nicola Vitulo[6], Mirco D'Agnolo[7], Raffaella Colombatti[7], Maddalena Martella[7], Maria Paola Boaro[7], Elena Doriguzzi Breatta[1,2], Anna Fregnani[1,2], Zaira Spinello[1,2], Mitja Nabergoj[8], Odile Filhol[9], Brigitte Boldyreff[10], Mattia Albiero[11,12], Gian Paolo Fadini[12,13], Carmela Gurrieri[1,2], Fabrizio Vianello[1,2], Gianpietro Semenzato[1,2], Sabrina Manni[1,2], Livio Trentin[1,2], Francesco Piazza[1,2]

Correspondence: Francesco Piazza (francesco.piazza@unipd.it).

ABSTRACT

The Ser-Thr kinase CK2 plays important roles in sustaining cell survival and resistance to stress and these functions are exploited by different types of blood tumors. Yet, the physiological involvement of CK2 in normal blood cell development is poorly known. Here, we discovered that the β regulatory subunit of CK2 is critical for normal hematopoiesis in the mouse. Fetal livers of conditional CK2β knockout embryos showed increased numbers of hematopoietic stem cells associated to a higher proliferation rate compared to control animals. Both hematopoietic stem and progenitor cells (HSPCs) displayed alterations in the expression of transcription factors involved in cell quiescence, self-renewal, and lineage commitment. HSPCs lacking CK2β were functionally impaired in supporting both in vitro and in vivo hematopoiesis as demonstrated by transplantation assays. Furthermore, KO mice developed anemia due to a reduced number of mature erythroid cells. This compartment was characterized by dysplasia, proliferative defects at early precursor stage, and apoptosis at late-stage erythroblasts. Erythroid cells exhibited a marked compromise of signaling cascades downstream of the cKit and erythropoietin receptor, with a defective activation of ERK/JNK, JAK/STAT5, and PI3K/AKT pathways and perturbations of several transcriptional programs as demonstrated by RNA-Seq analysis. Moreover, we unraveled an unforeseen molecular mechanism whereby CK2 sustains GATA1 stability and transcriptional proficiency. Thus, our work demonstrates new and crucial functions of CK2 in HSPC biology and in erythropoiesis.

INTRODUCTION

Hematopoiesis is a finely tuned developmental process regulated by cell-intrinsic (epigenetic, gene transcription) and extrinsic (cytokines, chemokines, and growth factors) mechanisms/molecules.[1,2] Signals generated by Stem cell factor (Scf)-cKit axis[3] and Erythropoietin-Receptor (EPO-R)[4] are fundamental for hematopoietic stem/progenitor cell (HSPC) growth and for red blood cell (RBC) production, respectively, through the activation of shared pathways, such as ERK/MAP kinases, JAK/STAT and PI3K/AKT signaling cascades. The EPO-R signaling culminates in the activation of the transcription factor GATA1[4–6] which sustains erythroid cell viability,[6,7] the switching from embryonic/fetal to adult globin chains,[8] heme biosynthesis[9] and supports also its own and *Epo-R*[10] transcription.

Protein kinase CK2 is a Ser/Thr kinase constituted by a tetramer of 2 catalytic (α or α')[11] and 2 regulatory (β) subunits, with CK2β being essential for the assembly of the kinase in a tetramer and for the selection of phospho-targets.[12] However, the α and β subunits exert also functions independently from the holoenzyme[12] and, importantly, free β dimers can bind and

[1]Department of Medicine, Division of Hematology, University of Padova, Italy
[2]Laboratory of Normal and Malignant Hematopoiesis and Pathobiology of Myeloma and Lymphoma. Veneto Institute of Molecular Medicine (VIMM), Padova, Italy
[3]Division of Hematology/Oncology, Boston Children's Hospital, Harvard Medical School, Boston, MA, USA
[4]Department of Medical Oncology, Dana-Farber Cancer Institute, Boston, MA, USA
[5]Department of Medicine, Cytopathology and Surgical Pathology Unit, University of Padova, Italy
[6]Department of Biotechnology, University of Verona, Italy
[7]Department of Women's and Child's Health, University of Padova, Italy
[8]Hematology Service, Institut Central des Hôpitaux (ICH), Hôpital du Valais, Sion, Switzerland
[9]Institut National de la Santé Et de la Recherche Médicale (INSERM) U1036, Institute de Reserches en Technologies et Sciences pour le Vivant/Biologie du Cancer et de l'Infection, Grenoble, France
[10]Kinase Detect, Krusaa, Denmark
[11]Department of Surgery, Oncology and Gastroenterology, University of Padova, Italy
[12]Veneto Institute of Molecular Medicine, Experimental Diabetology Lab, Padova, Italy
[13]Department of Medicine, University of Padova, Italy

HemaSphere (2023) 7:12(e978).
http://dx.doi.org/10.1097/HS9.0000000000000978.
Received: April 5, 2023 / Accepted: September 25, 2023

stabilize other proteins.[13] CK2 is involved in cell proliferation, resistance to stress, as well as many other processes.[14] One main property of CK2 is to sustain cell viability, hampering apoptosis by inhibiting procaspase-2 and caspase 8 and regulating BCL-2 family members.[15] In particular, CK2 prevents the activation of pro-apoptotic BID and enhances the expression of anti-apoptotic BCL-XL.[16] In addition, this kinase positively regulates survival pathways, such as NF-κB (in which it activates p65/RelA through phosphorylation in S529[17] and enhances IκBα[18] degradation and PI3K/AKT (through the inhibition of the phosphatase PTEN[19] and the activation of AKT[20,21]). We and others have demonstrated that CK2 is essential for acute myeloid leukemia (AML) and AML-derived leukemic stem cells,[22,23] multiple myeloma[24–26] and non-Hodgkin B cell lymphoma[27–30] cell survival, proliferation, and resistance to several intrinsic and extrinsic stresses.[31]

Since literature has also widely reported the key role of CK2 in embryogenesis,[32–34] we hypothesized that this kinase might also be essential for the ontogenesis of blood cells. In a recent article published by our group, we have demonstrated the importance of CK2 in B cell commitment towards follicular fate and in the germinal center reaction using mice bearing loxP-flanked CK2β alleles and expressing the Cre recombinase under the control of the *CD19* promoter.[35] In the present work, we crossed the same model of loxP mice with animals expressing the Cre recombinase under the control of the *Vav1* promoter, thereby achieving CK2β KO in all the hematopoietic cells. We focused the analysis on the HSPC and erythroid compartments.

CK2β KO during hematopoiesis dramatically affected mouse HSPC numbers and function ex vivo and in vivo. Mechanistically, we provided evidence that CK2β influences the expression of multiple transcription factors implicated in HSPC biology. Also, by exploiting an in vitro model of erythroid differentiation, we showed that CK2β is an essential stage-specific regulator of RBC differentiation, proliferation, and viability and we unraveled a molecular crosstalk between this kinase and the transcription factor GATA1.

METHODS

Mice

C57BL/6 VAV1-CRE mice were purchased from Jackson Laboratory, C57BL/6 *Csnk2b 2loxP* mice were described in,[34] C57BL/6 LY5.1 (CD45.1) mice were purchased from Charles River. Mice were kept in a pathogen-free colony at the animal facility of the Veneto Institute of Molecular Medicine, Padova, Italy. The University of Padova organization in charge for animal wellness approved the experimentation and declared that it fulfilled the National and European rules for animal studies. All the experimental procedures were authorized by the Italian Ministry of Health (Protocol N° 126-2015 and 205/2022-PR). For details on mice breeding, genotyping, and sample processing, see Suppl. Materials and Methods.

Repopulation assay

In competitive transplantation, CD45.1 mice were used both as recipient and competitor cells. Females, in synchronized gestations, were sacrificed at 14.5dpc; mixtures of equal amounts ($1x10^6$ cells) of donor (either *Vav1*$^{+/Cre}$ control or *Csnk2b*$^{fl/fl}$/*Vav1*$^{+/Cre}$ KO from CD45.2$^+$ genetic background) and wild-type competitor (CD45.1$^+$) total fetal liver cells were intravenously injected in lethally γ-irradiated (900rad) CD45.1$^+$ recipient mice. In non-competitive transplantation assay, CD45.1 recipient mice were injected only with (1×10^6 cells) CD45.2$^+$ cells from either *Vav1*$^{+/Cre}$ control or *Csnk2b*$^{fl/fl}$/*Vav1*$^{+/Cre}$ KO. Engraftment was assessed at 13/14 days for both experimental assays and after 1 month for competitive experiments in PB, BM, Spleen, Thymus, and Lymph Nodes. Repopulation efficiency of donor and competitor populations was investigated through fluorescence activated cell sorting (FACS) analysis after staining of PB or smashed hematopoietic tissues with Fc Block, anti-CD45.1, and anti-CD45.2 antibodies followed by erythrocyte cell lysis.

Cell culture and chemicals

G1E-ER cells, a kind gift of Prof. M. Weiss (St. Jude Childrens' Hospital, Memphis, TN) were maintained as described in.[36] Erythropoietin and 1-Thioglycerol were purchased from Sigma (Mo), SCF from Peprotec (UK). For cell treatment, β-estradiol (Merck) was used at 0.2 μM, CX-4945 (Activate Scientific GmbH) at 2.5 μM, Z-VAD-FMK (SelleckChem) caspase inhibitor at 5 μM, proteasome inhibitor bortezomib (SelleckChem) at 5 nM and cycloheximide (Merck) at 0.4 μg/ml.

RNA-Seq

The sequencing was performed on TER119$^+$ cells purified from 14.5 dpc fetal livers by FACS sorting. The complete RNA-Seq data are available in the Gene Expression Omnibus (GEO) (http://www.ncbi.nlm.nih.gov/geo) under accession number GSE158665. For the complete list of differently expressed genes see Suppl. Tables S1 and S2. For further details on the analysis methods, see SDC file.

Statistical analysis

Data were analyzed with the 2-tailed unpaired Student's *t*-test. Values were considered statistically significant at *P* values below *0.05, **0.01, ***0.001.

For further Materials and Methods, see the Supplemental Digital Content file.

Data availability

All data required to produce the results of this study are provided within the article, via supplemental files or with link to the dataset GEO with the accession number. Also included in supplemental file Suppl. Tables S3 - S7 reporting in order: list of primers for genotyping, qRT-PCR primers, antibodies for WB and flow cytometry, hemochrome of adult mice.

RESULTS

CK2β loss in the hematopoietic compartment is embryonic lethal and alters hematopoietic cell number, viability, and proliferation

We generated conditional CK2β-deficient mice in Vav1-expressing cells. In utero lethality between 19.5 and 20.5 days post conception (dpc) was observed in 100% of CK2β KO embryos (*Csnk2b*$^{fl/fl}$;*Vav1*$^{+/Cre}$). Control mice (*Csnk2b*$^{+/+}$;*Vav1*$^{+/Cre}$) and CK2β heterozygous mice (*Csnk2b*$^{+/fl}$;*Vav1*$^{+/Cre}$) were viable and fertile. We therefore analyzed fetuses at 12.5, 14.5, and 17.5 dpc. CK2β KO fetuses were pale and hemorrhagic, in some cases with the appearance of *hydrops fetalis*, more evident at 17.5 dpc (Figure 1A). Analysis of CK2β mRNA (Figure 1B) and protein levels (Figure 1C) in the fetal liver, primary site of hematopoiesis at this stage,[37] and in the brain from 14.5 dpc fetuses showed complete *Csnk2b* deletion restricted to the hematopoietic tissue. No significant changes were observed in CK2α protein levels (Figure 1C). CK2β-null embryos displayed smaller fetal livers with reduced cellularity as compared to controls (Figure 1D). FACS analysis of the CD45$^+$ (leukocyte) and Ter119$^+$ (erythroid) markers showed a reduction in the percentage of erythroid cells in the CK2β KO mice, while the percentage of leukocytes appeared slightly increased as compared to control littermates (Figure 1E). A deepened analysis of the white cell compartment revealed an accumulation in percentages of granulocytes and monocytes/macrophages in CK2β KO embryos (Figure 1F and 1G, left panels) that could account for the increased frequency of CD45$^+$ cells; however, the absolute counts of Mac1$^+$Gr1$^+$ and Mac$^+$F4/80$^+$ populations

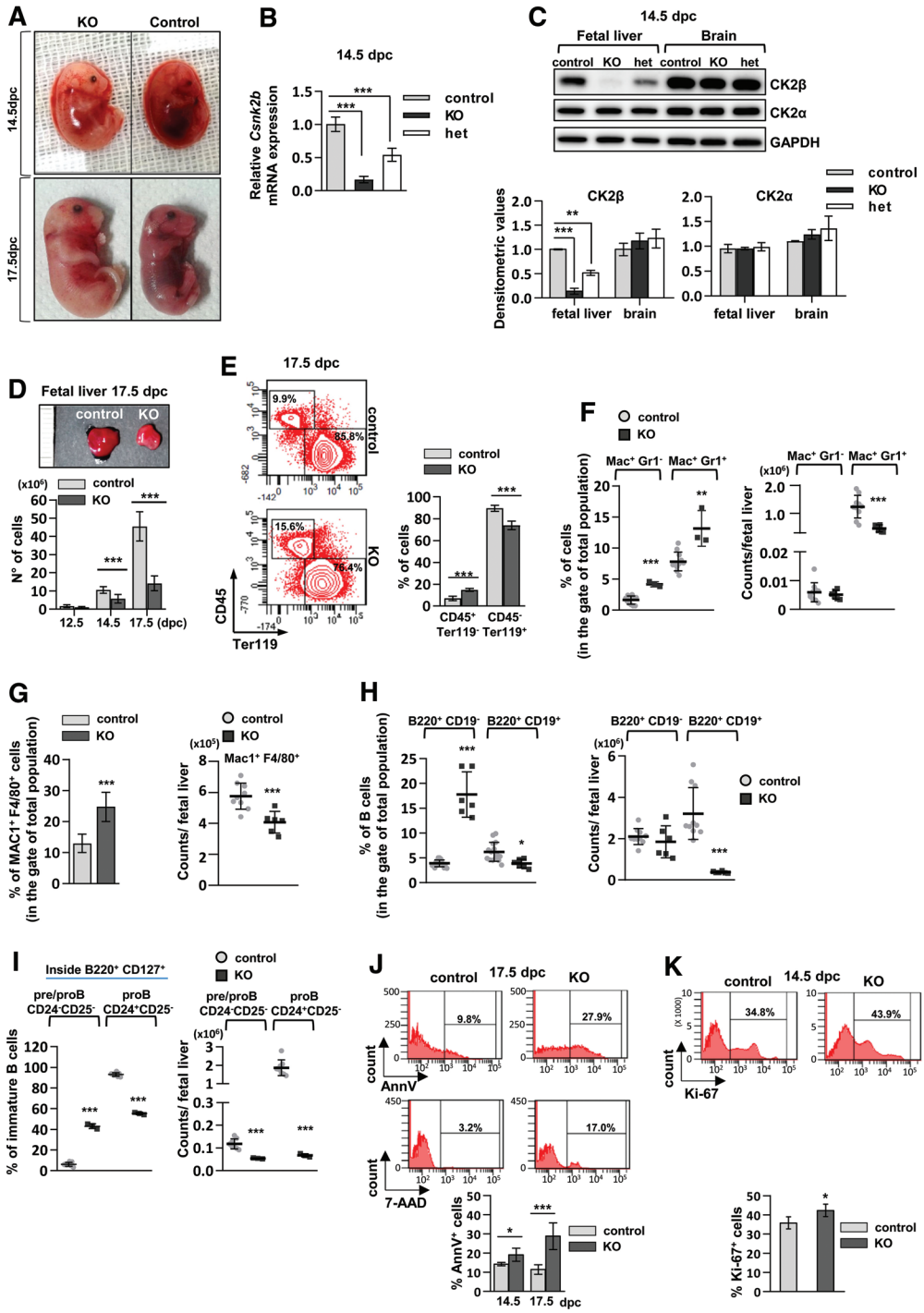

Figure 1. KO of CK2β in the fetal hematopoietic system results in embryonic lethality with reduction in fetal liver cellularity and alteration in cell viability and proliferation. (A) Pictures of *Csnk2b*$^{fl/fl}$/*Vav1*$^{+/Cre}$ (KO) and *Csnk2b*$^{+/+}$/*Vav1*$^{+/Cre}$ (control) littermate fetuses at 14.5 and 17.5 days post conception (dpc). (B) *Csnk2b* mRNA levels evaluated by qRT-PCR at 14.5 dpc in control and KO fetal livers. Data are representative of 5 samples for each genotype. *Gapdh* was used as reference gene. (C) WB analysis of CK2β and CK2α protein expression at 14.5 dpc in fetal liver cells compared to non-hematopoietic tissue (brain); upper panel: WB image representative of 4 samples for each genotype; lower panel: densitometric analysis; GAPDH was used as loading control. (D) Upper level: representative image of control and KO fetal livers at 17.5 dpc; lower level: fetal liver cell count at different development time points (12.5 dpc: controls n = 9, KO n = 6; 14.5 dpc controls n = 17, KO n = 18; 17.5 dpc: controls n = 18, KO n = 21). (E) FACS analysis of the white population (CD45$^+$) and erythroid cells (Ter119$^+$) in fetal livers at 17.5 dpc: on the left representative contour plot, on the right histograms displaying the percentages of the 2 hematopoietic compartments (controls n = 8; KO n = 3). (F) Scatter plots representing percentages of cells (on the left; controls n = 11, KO n = 3) or absolute counts (on the right; controls n = 10, KO n = 6) after Gr1 and Mac1 staining and FACS analysis in 17.5dpc fetal livers. (G) FACS analysis of macrophages (Mac1$^+$F4/80$^+$) in 17.5 dpc fetal livers represented as percentage on the left (controls n = 3, KO n = 3) and as absolute counts on the right (controls n = 9, KO n = 6). (H) Graphs indicating the percentages (on the left) (controls n = 15, KO n = 6) and absolute counts (on the right) (controls n = 10, KO n = 6) of B cells in 17.5dpc fetal livers. (I) FACS analysis of precursors B cells in 17.5 dpc fetal livers: graphs indicating the percentages (on the left) and absolute counts (on the right) (controls n = 8, KO n = 3). (J) Evaluation of apoptosis at 14.5 and 17.5 dpc by FACS analysis, after staining with Annexin V (AnnV) and 7-AAD, performed on total liver population (at 14.5 dpc controls n = 4, KO n = 5; at 17.5 dpc controls n = 20, KO n = 6). (K) Analysis of Ki-67 expression in 14.5dpc total liver cells (controls n = 5, KO n = 3). In (C–K), graphs show means ± SD; Student's t-test: *$P < 0.05$; **$P < 0.01$; ***$P < 0.001$. FACS = fluorescence activated cell sorting; KO = knockout; WB = western blot.

in total fetal livers resulted to be reduced in the KO samples compared to the control ones (Figure 1F and 1G, right panels). Moreover, also the B cell compartment was altered in CK2β KO mice with accumulation in percentages of immature B cells ($B220^+$ $CD19^-$) (Figure 1H, left panel) and expansion of pre/pro B cells (Figure 1I, left panel). Also in this case the counts in the total fetal livers show discrepancies compared to the frequencies due to the reduced global cellularity of livers in KO embryos; indeed, there were no significant changes in $B220^+$ $CD19^-$ absolute numbers (Figure 1H, right panel) and there was a decrease of pre/pro cells in KO embryos (Figure 1I, right panel). Annexin V (AnnV) and 7-Aminoactinomycin D (7-AAD) staining revealed a higher percentage of apoptotic cells in CK2β KO fetal livers that became more evident at 17.5 dpc (Figure 1J). However, analysis of Ki-67 expression showed a mild increase in cell proliferation in CK2β KO compared to control mice (Figure 1K).

Deletion of CK2β affects hematopoietic stem and progenitor cell proliferation kinetics and transcriptional programs

Next, we analyzed the immature hematopoietic compartment represented by stem (HSC) and progenitor cells (HPCs) evaluating the effects of *Csnk2b* ablation. FACS analysis of HSCs[38] and HPCs[39] revealed a significant increase in the percentages of HSCs (Lin^- $cKit^+$ $Sca\text{-}1^+$ $CD150^+$ $CD48^-$) (Figure 2A and 2D), MEPS (Lin^- $cKit^+$ $Sca\text{-}1^-$ $CD34^-$ $FcyRIII/II^-$), CMPs (Lin^- $cKit^+$ $Sca\text{-}1^-$ $CD34^+$ $FcyRIII/II^{low}$) and GMPs (Lin^- $cKit^+$ $Sca\text{-}1^-$ $CD34^+$ $FcyRIII/II^{high}$) (Figure 2B and 2D) in KO fetal livers compared to controls with no significant changes in CLPs (Lin^- $IL\text{-}7R^+$ $cKit^+$ $Sca\text{-}1^{-/low}$) (Figure 2C and 2D). However, analysis of absolute counts in the total fetal livers confirmed in the KO samples a significant expansion limited to the LSK compartment and a trend to higher counts for GMPs (Figure 2E). Notably, the intensity of cKit expression, a receptor essential for HSC and precursor survival and self-renewal, was found substantially reduced (mean fluorescence intensity, MFI) in CK2β KO HSPCs (Figure 2F).

Since during blood cell development proliferation and differentiation must be tightly coordinated, we analyzed the cell cycle of LSK cells, using BrdU and 7-AAD staining and FACS analysis. As shown in Figure 2G, a higher percentage of cells was in G2/M, S, and sub-G_0 phases and displayed a greater DNA content (gate >2n) in KO mice compared to controls.

We next inquired if CK2β loss could affect the expression of transcription factors important for HSC and HPC early lineage commitment. By qRT-PCR we evaluated the expression of specific mRNAs coding for transcription factors involved in cell maturation (*Gata1*,[5,40] *Jun*[41]) or in the maintenance of stem cell quiescence and self-renewal (*Scl*/Tal1,[42] *Bmi-1*,[43] *Runx1*,[44,45] *Pu.1*,[46] *Cebpa*,[47] *Gata2*[48]), in FACS-sorted LSKs, CMPs, GMPs and MEPs (Figure 2H). In CK2β KO embryos, the LSK compartment exhibited a reduced expression of *Scl/Tal1* and *Pu.1* with no significant changes in *Bmi-1* and *Runx1* mRNA levels compared to controls. Loss of CK2β caused a decrease of *Runx.1*, *Pu.1* and *Cepba* expression in CMPs and a decrease of *Cebpa* and *Gata1* in GMPs. MEPs from KO mice showed alterations in almost all the genes analyzed with a significant reduction of *Scl/Tal1*, *Bmi-1, Runx1,* and *Gata1* and an increase of *Jun* expression.

In summary, lack of CK2β causes an accumulation and increased proliferation of HSCs and an altered expression of transcription factors involved in the regulation of HSPC quiescence and commitment.

CK2β is essential for hematopoietic reconstitution capability in vitro and in vivo

To assess the differentiative potential of progenitors, we performed methylcellulose-based colony-forming assays of fetal liver HSPCs. Strikingly, KO cells displayed an impairment to generate erythroid and myeloid colonies at 3 and 6 days (Suppl. Figures S1A and S1B). In vivo competitive repopulation assays of 14.5 dpc fetal liver cell transplanted in C57BL/6 congenic mice expressing the differential leukocyte marker CD45.1 were then performed (Figure 3A).[49,50] As summarized in Table 1, an almost complete restoration of hematopoiesis was obtained as early as 2 weeks after transplantation with comparable blood cell percentages between mice injected with both kinds of cell mix. To note, FACS analysis of peripheral blood revealed an equal contribution to hematopoiesis when control $CD45.2^+$ and competitor $CD45.1^+$ donor cells were injected, while the injection of CK2β KO $CD45.2^+$ did not contribute to mature blood cells (Figure 3B). The same phenotype was observed after 4 weeks in all the hemo-lymphopoietic organs (Figure 3B–3D). We also evaluated the contribution to the generation of LSK and HSCs from $CD45.1^+$ and $CD45.2^+$ cell populations. Remarkably, in recipient mice injected with the competitive KO transplant there was a complete absence of CD45.2 expression both in LSK (Figure 3E) and in HSCs ($CD48^-CD150^+$ in LSK gated cells)[51] (Figure 3F). Since the lack of engraftment in the BM could be linked to a problem of homing of HSCs, we evaluated by FACS the expression of CXCR4 (a known key mediator of HSC homing to the bone marrow[52]) in LSK compartment of control and CK2β KO fetal livers (Figure 3G). Unexpectedly, CK2β KO embryos showed higher percentages of $CXCR4^+$ LSK cells and higher MFI of this marker as compared to control counterpart, suggesting that the observed phenotype is likely not dependent on this molecule. To exclude the possibility that the lack of KO cell engraftment was due to the inability of $CD45.2^+$ CK2β null LSK to compete with CD45.1 cells for the BM niches, we also performed non-competitive transplantation assays. As described in Suppl. Figure S1C, CD45.1 adult mice were irradiated and injected with only CD45.2 cells from control or KO fetal livers; 2 out of 5 mice injected with CK2β null $CD45.2^+$ cells died at day 12, thus we anticipated the experimental end point at 13 days. In all the compartments analyzed (SP, BM, and spleen) we evidenced almost the complete absence of CD45.2 cells from KO samples (Suppl. Figure S1D). Moreover, analysis of $CD45.2^+$ LSK frequencies and events in the BM (Suppl. Figure S1E) underlined that CK2β KO progenitors and stem cells were unable to engraft and sustain hematopoiesis.

Erythropoiesis is defective in CK2β KO mice

Deletion of CK2β in purified $Ter119^+$ mature erythroid cells was complete (Figure 4A). The levels of the catalytic α subunit were found decreased and a CK2-specific kinase assay showed a 60% residual enzymatic activity (Figure 4A), likely attributable to the remaining α dimers. FACS analysis of CD71 and Ter119 markers in fetal livers at 14.5 and 17.5 dpc[53,54] revealed that CK2β KO embryos had unbalanced frequencies of erythroid subfractions compared to control mice (Figure 4B). KO samples displayed accumulation of both $CD71^{low/-}$ $Ter119^-$ and $CD71^{high}$ $Ter119^-$ immature populations and, particularly at 17.5 dpc, depletion of the most mature $Ter119^+$ $CD71^-$ fraction (Figure 4B, left and middle panels). Analysis on pellets of peripheral blood obtained from 17.5 dpc embryos confirmed a reduced amount of mature hemoglobinized cells in CK2β KO samples (Figure 4B). Furthermore, KO fetal liver cells presented a reduced expression of both Ter119 and CD71 (Figure 4B, right panels). Similarly to the HSPCs, the MFI of cKit expression was found reduced in CK2β-deficient $CD71^+Ter119^{-/low}$ population mainly composed of CFU-E, BFU-E and pro-Erythroblasts (Figure 4C). Complete blood cell count analysis performed on peripheral blood of 17.5 dpc embryos pointed out a strong reduction of RBC counts in KO samples (Figure 4D). To further support the evidence of terminal erythroid maturation impairment, since the extrusion of the nucleus is one central step of erythrocyte production, we evaluated the amount of nucleated and anucleated erythroid cells within the gate of $Ter119^+$ FSC^{low} cells.[55,56] The nuclear staining through Syto-16 tracker evidenced

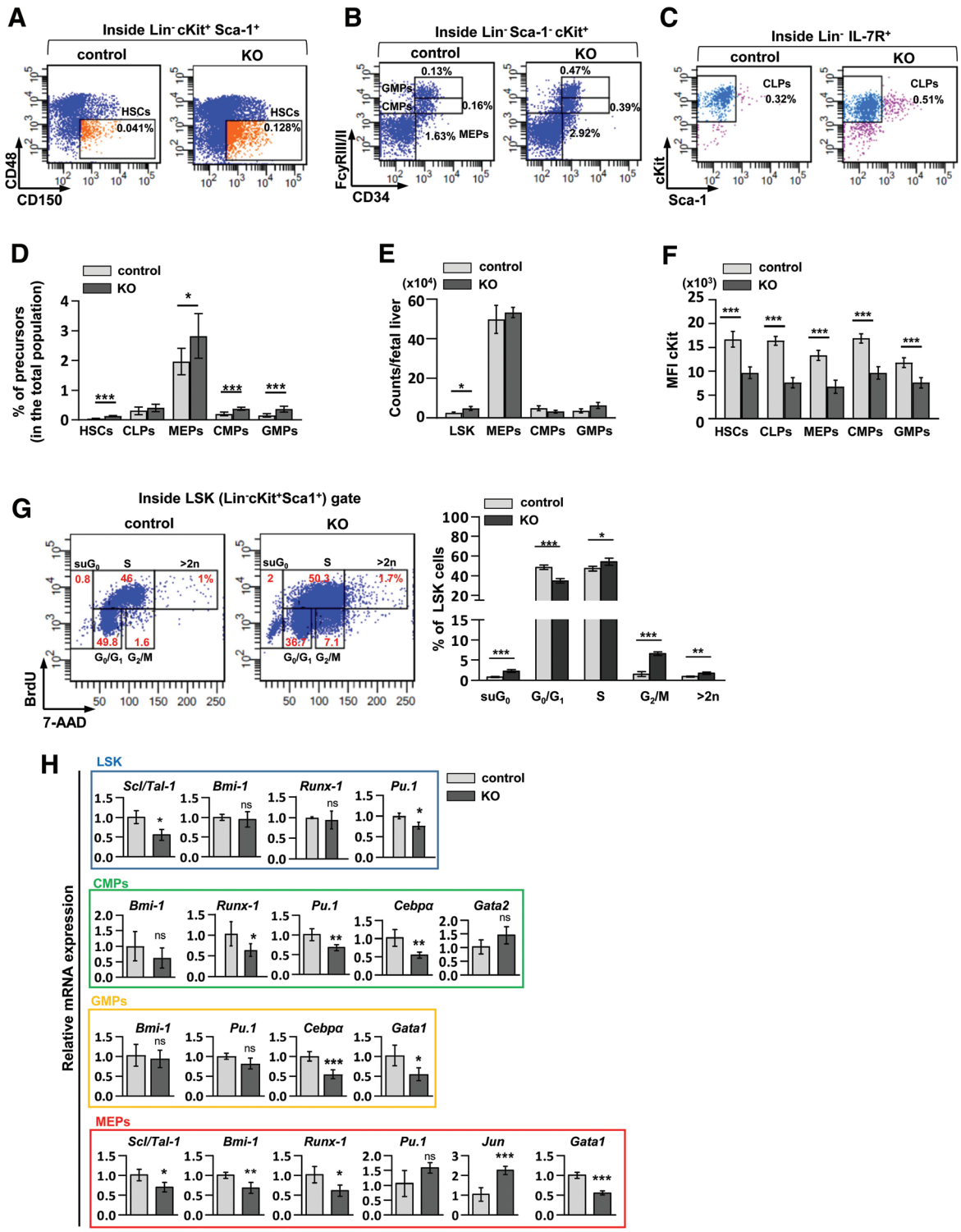

Figure 2. Absence of CK2β increases the amount of hematopoietic stem cells and precursors and perturbs their maturation program. Representative FACS dot plot of hematopoietic stem cells (HSCs) (A), common myeloid progenitors (CMPs), megakaryocyte/erythrocyte progenitors (MEPs), granulocyte/monocyte progenitors (GMPs) in 14.5 dpc fetal livers (B), common lymphoid progenitors (CLPs) (C); the representative dot plots show the percentage of cells; $1x10^6$ and at least 4×10^5 events were acquired for LT-HSCs and the other progenitors respectively. (D) Histogram summarizing the percentages of each population (for HSC controls n = 5, KO n = 4; for the other precursors: controls n = 9, KO n = 6). (E) Graphs representing absolute cell counts of LSK, MEPs, CMPs, and GMPs populations referred to the total fetal liver (controls n = 3, KO n = 3). (F) Histograms exhibiting mean fluorescence intensity (MFI) in HSCs and each precursor sub-population (controls n = 9, KO n = 6). (G) BrdU proliferation assay in 14.5 dpc fetal livers cells: cell cycle was analyzed inside the LSK ($Lin^-Sca\text{-}1^+cKit^+$) fraction after staining with anti-BrdU and 7-AAD. Left panel: representative contour plots and gating strategy; right panel: histograms summarizing the percentages of the cells in each stage (controls n = 4, KO n = 4). (H) qRT-PCR showing the relative mRNA expression of *Scl/Tal1, Bmi-1, Runx1, Jun, Pu.1, Cebpa, Gata1, Gata2* genes in HSCs (controls n = 3, KO n = 3), CMPs (controls n = 4, KO n = 5), GMPs (controls n = 4, KO n = 5) and MEPs (controls n = 4, KO n = 5) purified through sorting from 14.5dpc fetal livers. *Gapdh* was used as reference gene. In all panels (D–H) the graphs report mean ± SD values; Student's t-test: $^*P < 0.05$; $^{**}P < 0.01$; $^{***}P < 0.001$. CLPs = common lymphoid progenitors; CMPs = common myeloid progenitors; FACS = fluorescence activated cell sorting; GMPs = granulocyte/monocyte progenitors; HSCs = hematopoietic stem cells; KO = knockout; LSK = Lin-Kit+Sca1+; MEPs = megakaryocyte/erythrocyte progenitors.

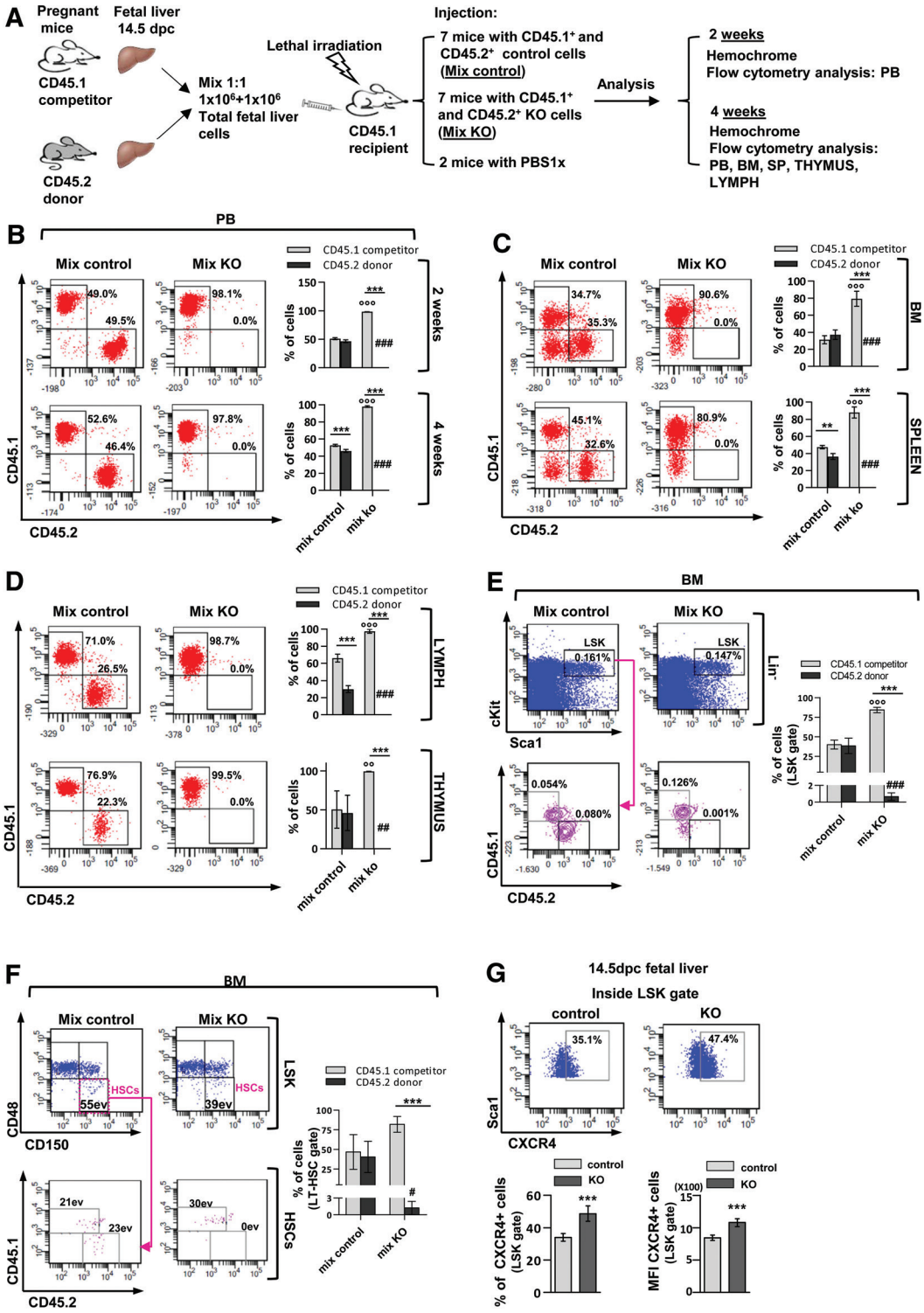

Figure 3. Fetal liver cell transplantation from KO fetuses in recipient adult mice results in the lack of hematopoietic reconstitution. (A) Transplant workflow: a mixed population with equal proportions of CD45.2 (donor from control or KO) and CD45.1 (competitor) fetal liver cells were injected in recipient CD45.1 adult mice after lethal total body irradiation (900 rads). The transplantation with CD45.2 cells from control embryos plus CD45.1 competitor cells is indicated as Mix Control; when CD45.2 cells were obtained from CK2β-null embryos plus CD45.1 competitor cells, the injected population is called Mix KO. Hematopoietic restoration was assessed at 2 and 4 weeks from irradiation. Injection of PBS was used as control of irradiation efficacy. Sample size: 7 mice injected with mix control, 7 with mix KO, and 2 with PBS. (B–F) Flow cytometry analysis of CD45.2 and CD45.1 relative amounts in (B) peripheral blood (PB), (C) bone marrow (BM), spleen (SP), and (D) lymph nodes and thymus, (E) inside the gate of LSK and (F) inside long term HSCs. On the left of each figure are depicted the representative dot plots and on the right are the histograms with CD45.1 and CD45.2; (G) Flow cytometry analysis of CXCR4 expression in 14.5 dpc fetal livers; upper panel: representative dot plots; lower panel: histograms representing the percentages and mean fluorescence intensities (controls n = 5, KO n = 3). Data in the graphs (B–G) are shown as mean ± SD, Student's t-test: $^{*}P < 0.05$, $^{**}P < 0.01$, $^{***}P < 0.001$ comparing donor CD45.2 vs competitor CD45.1; $^{\circ\circ}P < 0.01$, $^{\circ\circ\circ}P < 0.001$ comparing CD45.1 population from KO mix vs that one of control mix; $\#P < 0.05$, $\#\#P < 0.01$, $\#\#\#P < 0.001$ comparing CD45.2 population from KO mix vs that one of control mix. BM = bone marrow; HSCs = hematopoietic stem cells; KO = knockout; LSK = Lin-Kit+Sca1+; PB = peripheral blood; PBS = phosphate buffered saline; SP = spleen.

Table 1

Hemochrome of Transplanted Mice

	2 wks		4 wks	
Parameters	**CTRL**	**KO**	**CTRL**	**KO**
WBC (10^3/μL)	2.87 ± 0.70	2.60 ± 0.35	9.83 ± 1.53	7.17 ± 1.24**
RBC (10^6/μL)	10.12 ± 0.32	8.11 ± 1.73	12.00 ± 1.87	10.80 ± 0.67
HGB (g/dL)	15.00 ± 0.53	11.80 ± 3.12	15.87 ± 2.13	14.73 ± 0.86
HCT (%)	42.33 ± 1.62	34.67 ± 9.27	49.30 ± 7.75	44.77 ± 2.78
MCV (fL)	41.90 ± 0.92	42.40 ± 3.00	41.05 ± 0.28	41.43 ± 0.29*
PLT (10^3/μL)	1062.00 ± 419.24	650.00 ± 68.79	1842.67 ± 152.39	1764.00 ± 151.61
MPV (fL)	7.00 ± 0.66	8.90 ± 1.10	5.07 ± 0.38	5.07 ± 0.38
LYM%	51.73 ± 8.35	61.03 ± 3.65	75.80 ± 5.36	70.85 ± 5.59
MID%	10.07 ± 1.79	6.73 ± 1.94	9.55 ± 0.94	12.27 ± 2.37*
GRA%	38.20 ± 6.56	32.23 ± 2.40	14.65 ± 5.99	16.88 ± 3.46

*$P < 0.05$;

**$P < 0.01$ compared to mice injected with cells from control embryos.

CTRL = controls; GRA = granulocytes; HCT = hematocrit; HGB = hemoglobin; KO = knockout; LYM = lymphocytes; MCV = mean corpuscolar volume; MID = monocytes; MPV = mean platelet volume; PLT = platelets; RBC = red blood cell; WBC = white blood cell.

a higher percentage of nucleated cells (Syto-16$^+$) with parallel reduction of enucleated cells (Syto-16$^-$) in KO samples compared to controls (Figure 4E). Cytospin preparations of Ter119$^+$ fetal liver cells (Figure 4F, upper panel) revealed dysplastic features with membrane irregularities and blebs (blue arrows) of immature erythroblasts in KO mice. Reticulocytes looked irregularly shaped with intracellular inclusions resembling in size and color (but not in number) the Howell-Jolly bodies (red arrows). Also, peripheral blood smears (Figure 4F, bottom panel) showed larger erythrocytes, which in some instances appeared swollen and vacuolized. Since these morphological alterations could rely on defects of red cell membrane properties, such as the ability to change shape under the effect of mechanical forces, we evaluated erythrocyte deformability capacity in 17.5 dpc embryos by means of an ektacytometer. As shown in Figure 4G, erythrocytes from peripheral blood of KO animals presented a significant reduction in the elongation index, thus less deformability, when they were exposed to a range of applied stress from 0.3 to 30 Pa.

Both fetal and adult CK2β heterozygous (het) mice did not suffer an anemic condition: for detailed description of their erythroid phenotype, see Suppl. Figure S2, S Results and Suppl. Table S7 that reports the hemochrome values.

Thus, loss of CK2β results in abnormal erythroid maturation, with reduction of terminally differentiated cells.

CK2β regulates erythroid cell survival and proliferation by impinging on multiple intracellular pathways

To understand the mechanism underlying deficient erythroid maturation, we evaluated apoptosis by AnnV and 7-AAD staining (Figure 4H). The mature Ter119$^+$ population from KO mice presented, as early as 14.5 dpc and to a higher extent at 17.5 dpc, an increase of cells in late-stage apoptosis (AnnV$^+$/7-AAD$^+$) and necrosis (AnnV$^-$/7-AAD$^+$) as compared to controls. On the contrary, the immature CD71$^+$Ter119$^-$ fraction did not present significant alterations in cell viability. WB analysis of Ter119$^+$ purified cells (Figure 4I) revealed in CK2β-deficient cells a significant decrease of PRO-CASPASE-3 with accumulation of its active cleaved form, an increase of PARP cleavage and a reduction of BCL-xL, a BCL-2 family member pivotal for the survival of late stages erythroblasts. Investigation of other BCL-2 family members highlighted an up-regulation of the pro-apoptotic proteins BAX and PUMA in KO samples at both 14.5 and 17.5 dpc and the same trend was also observed for the anti-apoptotic factor MCL-1 that is reported be essential in immature erythroblasts and erythroid progenitors.[57] Moreover, 14.5 and 17.5 dpc fetal liver KO cells expressed markedly higher levels of the TP53 downstream target P21 (Figure 4I).

To assess the proliferation kinetics, we performed an in vivo BrdU incorporation assay. FACS analysis showed a reduction of CD71$^+$ Ter119$^-$ immature cells in the S phase and an increase of Ter119$^+$ mature cells in the subG$_0$/G$_1$ phase without significant changes in S and G$_2$/M phases, in KO mice compared to CTRL (Figure 4J).

Next, we carried out RNA-Sequencing in Ter119$^+$ fetal liver cells. As many as 1143 differentially expressed genes were identified in CK2β-null mice as compared to controls (See Suppl. Tables S1 and S2 for the complete list of up and down-modulated genes respectively). Pathway enrichment analysis revealed in KO samples (Figure 5A) an up-regulation of some P53-targets, such as *Cdkn1a (P21), Zmat,* and *Gadd45*, a deregulation of genes associated with the JAK/STAT pathway, in particular a down-modulation of *Stat5,* essential for erythroid cell viability,[58] and overexpression of *Socs2,* coding for an inhibitor of this signaling cascade.[59] Moreover, we observed a down-regulation of *Kit* and of genes associated to the PI3K/AKT pathway such as *Pi3kr1* and *Gab1*. Interestingly, there was the up-regulation of *Jun,* co-factor of PU.1, known to inhibit erythroid differentiation counteracting the transcriptional capability of GATA1, the master regulator of terminal erythroid maturation.[5] Another dysregulated gene category was the group of solute carrier transporters (*Slc*) implicated in ion homeostasis.[60] Intriguingly, mRNA expression of *Siglec1*, *Vcam1*, and *Selplg* were decreased in KO samples. These are markers expressed by macrophages of the erythroblastic islands[61] and it was described in a recent work that a contamination of these cells is frequently observed in purified Ter119 fraction because of the tight connection between erythroid and macrophage populations.[62] We therefore validated by qRT-PCR the expression of some of the deregulated genes identified by RNA-Seq (genes highlighted in yellow). Analysis was performed at 17.5 dpc (Figure 5B) and 14.5 dpc (Suppl. Figure S3A) on Ter119$^+$ fetal liver cells. A complementary analysis obtained interrogating RNA-seq data with Gene Ontology terms of our interest (see Supplemental material for details on the analysis) showed in KO samples the significant deregulation of other 114 genes (Suppl. Figure S3B) involved in erythroid cell membrane stability (*Ebp4.1*-pink highlighted), water homeostasis (*Aqp1*-green highlighted[63]), heme biosynthesis (*Tmem14c*-violet highlighted), and in particular genes related to the mitotic process (blue highlighted genes). Furthermore, we evaluated the deregulation in expression of genes coding for kinases, confirming the down-regulation of *Csnk2b* in KO samples (Suppl. Figure S3C, top), and of genes coding for transcription factors, showing a reduction in KO cells of *Ikzf1* (Ikaros1) and *Klf13,* both involved in erythroid maturation (Suppl. Figure S3C, bottom).[64,65]

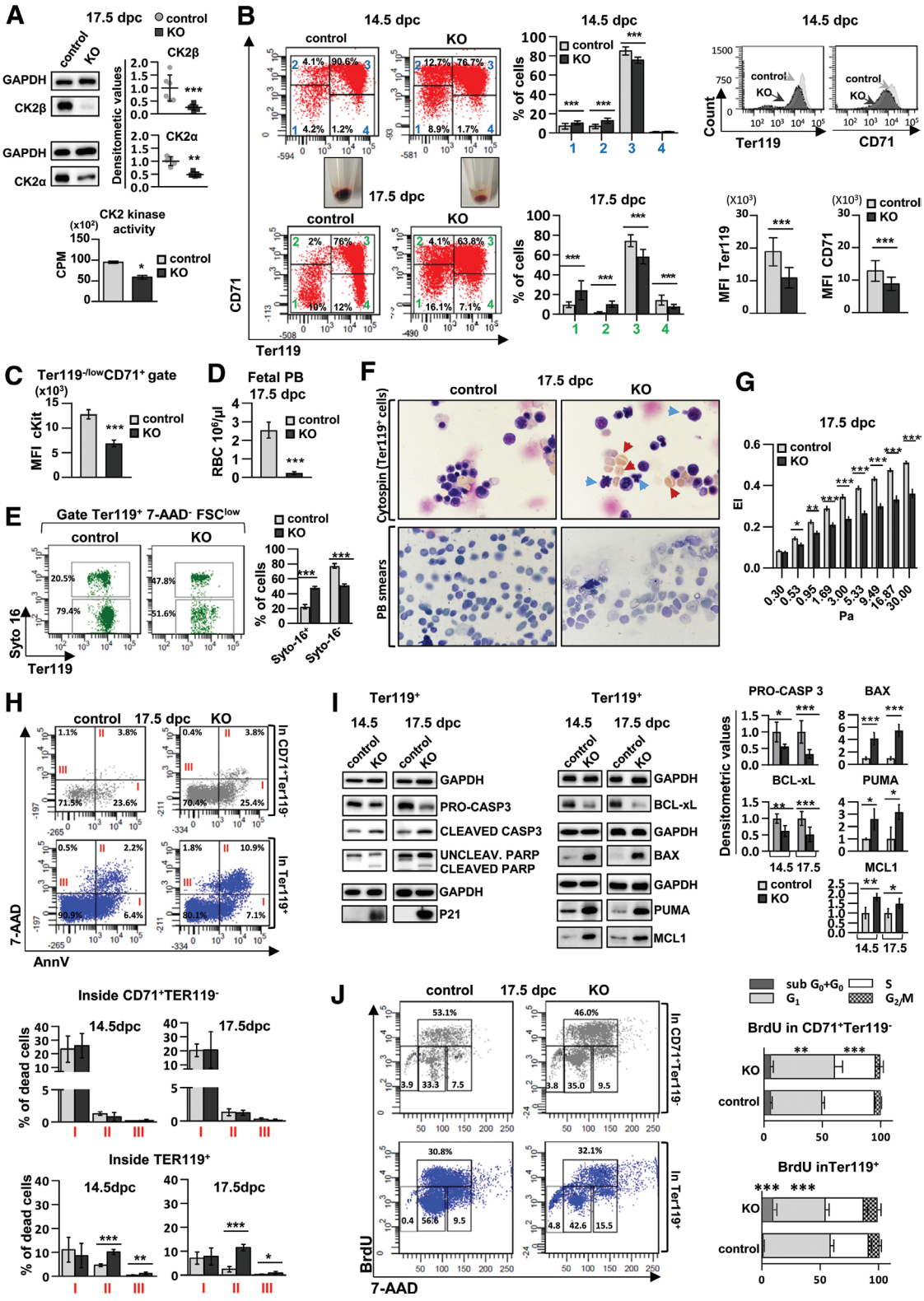

Figure 4. Ablation of *Csnk2b* in the hematopoietic compartment causes ineffective erythropoiesis with red blood cell morphological alteration, impairment of cell viability, and unbalance in cell proliferation. (A) Top: WB analysis of CK2β and CK2α expression; bottom: CK2 kinase activity displayed as count per minute (CMP) in Ter119+ cells from 17.5 dpc fetal livers. (B) Study of erythroid maturation stages by FACS at 14.5 and 17.5 dpc, analyzing transferrin receptor (CD71) and glycophorin-associated protein Ter119. In detail: (B) left panel: representative dot plot with the gating strategy and sub-populations 1 (Ter119^{-}CD71$^{-/low}$), 2 (Ter119^{-}CD71^{high}), 3 (Ter119^{+}CD71^{high}) 4 (Ter119^{+}CD71$^{-/low}$) and representative pellets of peripheral blood samples from 17.5dpc embryos; middle panel: histograms summarizing percentages of each erythroid sub-population; right panel: peaks and graphs showing Ter119 and CD71 expression represented as mean intensity fluorescence (MFI). Sample size: n = 19 controls and 9 KO at 14.5 dpc; n = 20 controls and 6 KO at 17.5 dpc. (C) MFI of cKIT in the gate of Ter119$^{-/low}$ CD71^{+} cells (14.5dpc fetal livers; n = 16 controls and n = 7 KO). (D) Red blood cell counts (RBC) in the peripheral blood of 17.5 dpc embryos (n = 7 controls, n = 3 KO). (E) Evaluation of nucleated and enucleated erythroid cells through Syto-16 staining. Left, contour, and dot plots (*Continued*)

Figure 4 Continued. showing the gating strategy; right, graphs summarizing the percentages of nucleated (Syto-16$^+$) and enucleated (Syto-16$^-$) cells in control and KO erythroid cells. Sample size: n = 3 controls and n = 3 KO. (F) Upper panel: cytospin of Ter119$^+$ cells purified from fetal livers; lower panel peripheral blood smears from 17.5 dpc fetuses. Samples stained with May-Grunwald Giemsa. Red arrows indicate cells with membrane blebs, and blue arrows indicate abnormal reticulocytes. Sample size: data are representative of 4 controls and 4 KO, at least 3 images were acquired for each sample. (G) Histogram representing the deformability of red blood cells in 17.5 embryos; test performed using Lorca ektacytometer on whole peripheral blood. Rigidity and plasticity are evaluated as Elongation Index (EI); deformability was assessed over a range of shear stresses between 0.3 and 30 Pa. Sample size: data are representative of 14 controls and 6 KO. Results were expressed as means ± SEM. Multiple t-tests were corrected with Holm-Sidak method: *P < 0.05, **P < 0.01, ***P < 0.001. (H) Evaluation of apoptosis at 14.5 and 17.5 dpc by flow cytometry analysis, after staining with Annexin V (AnnV) and 7-AAD; analysis was performed on erythroid sub-populations (CD71$^+$Ter119$^-$) and (Ter119$^+$); top panel: representative dot plot, bottom panel: histograms showing cell percentages. Sample size: controls n = 8, KO n = 4 at 14.5 dpc; controls n = 9, KO n = 4 at 17.5 dpc. (I) WB of CASPASE-3, PARP, the anti-apoptotic BCL-xL, and the P53 downstream target P21 levels. Sample size: n = 4 controls and 4 KO at 14.5 dpc; 12 controls and 13 KO at 17.5 dpc). For BAX, MCL-1, and PUMA the sample size was composed of n = 3 controls and 3 KO at 14.5 dpc; n = 6 controls and 5 KO at 17.5 dpc. (J) Analysis of cell cycle stages in erythroid sub-populations after anti-BrdU and 7-AAD staining combined with Ter119/CD71 markers. Sample size: n = 6 controls and 5 KO. In (A–E) and (H–J), graphs report means ± SD. In (A) and (I) densitometric analysis, data were normalized over GAPDH and over the mean value of controls. Student's t test: *P < 0.05, **P < 0.01, ***P < 0.001. EI = elongation index; FACS = fluorescence activated cell sorting; KO = knockout; RBC = red blood cell counts; WB = western blot.

CK2β-deficient erythroid cells show deregulated cell signaling and GATA1 activity

Since EPO-R is essential in driving erythroid maturation from pro-erythroblast to late stages, we investigated the signaling upstream and downstream of this receptor. ELISA performed on plasma obtained from 17.5 dpc embryos showed a trend for lower EPO levels in CK2β KO samples (Figure 5C). EPO-R protein levels on Ter119$^+$ purified cells resulted unaltered in KO mice compared to controls (Figure 5D). Next, we analyzed downstream JAK/STAT, ERK, PTEN, and PI3K/AKT signaling cascades,[4] this latter culminating in the AKT-directed phosphorylation of GATA1 on Ser310 that empowers its transcriptional activity.[66] Immunoblot analysis on Ter119$^+$ fetal liver cells (Figure 5E) revealed markedly decreased levels of total AKT and GATA1 at both 14.5 and 17.5 dpc and of STAT5, ERK1/2 (p44-42) at 17.5 dpc. However, their phosphorylation at CK2-independent or indirectly regulated (ie, AKT S473) sites was not significantly affected when the quantification was normalized against the total protein level, as opposed to the phosphorylation of residue AKT S129[67] (direct CK2 target) which is clearly reduced in KO cells. PTEN showed a significant decrease of the inhibitory phosphorylation on Ser380/Thr382/383, both at 14.5 and 17.5 dpc and a depletion in total protein levels at later time points in CK2β KO mature erythroid cells. Moreover, KO samples displayed a higher phosphorylation, thus activation, of SAPK/JNK kinases, which are involved in stress signaling and in the activation of the transcription factor c-JUN (Suppl. Figure S3D). Consistently, KO mice exhibited reduced mRNA levels of the GATA1 target genes *β-globin*,[8] *Lrf/Zbtb7a*[7], and *Klf*[5] transcription factors and of *Alas2*,[9] which encodes for 5'-aminolevulinate synthase 2, the enzyme catalyzing the first reaction in heme biosynthesis (Figures 5F and S3E). As a further expected consequence of GATA1 down-modulation, we observed the up-regulation of the ε embryonic (β-like) globin chain and of *Gata2* transcription factor (Figures 5F and S3E). Validation of these findings was also performed at the protein level for ALAS2 and LRF (Figure 5G). Moreover, the low levels of GATA1 could also explain the deregulated expression of *Slc* genes observed in the RNA-seq analysis since they are reported to be controlled by this transcription factor.[60,63]

Importantly, in KO samples also FOG1, a key co-factor of GATA1 essential for both erythropoiesis and megakaryopoiesis,[63,68] was down-regulated (Figure 5G). Additionally, Prussian blue staining on fetal liver sections clearly showed the presence of reactive ferric iron deposits in CK2β-null mice, likely due to Alas2 deficiency[69] (Suppl. Figure S3F).

cKit receptor is known to sustain immature erythroid cells, such as BFU-E, and to cooperate with EPO-R in maintaining CFU-E and pro-erythroblasts. Since we demonstrated that cKit is down-regulated also in these populations (included in Ter119$^{-/low}$CD71$^+$ gate) (Figure 4C), we asked whether erythroid linage impairment could be partly due to a less effective cKit signaling. CD71$^+$Ter119$^{-/low}$ fraction was isolated through sorting from 14.5 dpc pools of control or KO fetal livers (Figure 5H left panel, gating strategy). Then, cells were treated with SCF for 15 minutes to evaluate the activation of 2 key effectors downstream Kit, that is, ERK and AKT. WB analysis revealed a severe reduction of both ERK and AKT phosphorylation in KO samples compared to controls (Figure 5H, middle and right panels).

Altogether, these results clearly suggest that CK2 regulates erythropoiesis by controlling signaling pathways downstream EPO-R, and in particular regulating GATA1 levels and transcriptional proficiency, as well as the modulation of cKit expression and its downstream targets.

CK2 regulates GATA1 expression, localization, and turnover during erythroid differentiation

To understand the CK2-mediated mechanism of signaling and GATA1 regulation, we used the G1E-ER cell line, a model of β-estradiol-inducible GATA1-dependent erythroid differentiation.[36] G1E-ER cells were cultured with or without β-estradiol in the presence of CX-4945 (silmitasertib), a selective inhibitor of CK2 kinase activity.[70] Exposure to β-estradiol led to erythroid differentiation as indicated by the appearance of Ter119$^+$ CD71$^+$ cells (Figure 6A). G1E-ER cells can differentiate up to the orthochromatic erythroblast stage at most and after 72 hours of culture with β-estradiol they undergo apoptosis.[6,71–73] To note, the addition of silmitasertib caused a significant reduction of Ter119$^+$ cells and a decrease of CD71 expression. Importantly, cell viability remained comparable in treated and untreated samples up to 24 hours (Suppl. Figure S4A), while at 48 hours, only in the condition where silmitasertib was used as single treatment, cell viability was slightly reduced. Therefore, apoptosis was unlikely the cause of the reduction of differentiated cells in the combined treatment. Tetramethylbenzidine test (Suppl. Figure S4B) performed at 48 hours indicated a decreased content of hemoglobin in the combined treatment confirming the impairment of erythroid maturation. The same analysis was performed upon *Csnk2b* or *Csnk2a* knockdown by siRNA (Figure 6B). The silencing of both subunits, when combined with β-estradiol, produced a similar impairment of erythroid differentiation, while the decrease of CD71 MFI was observed also in the absence of β-estradiol (Figure 6B). AnnV analysis did not highlight significant changes in cell viability except for the condition of *Csnk2a* siRNA without β-estradiol, in which a mild increase in apoptosis was seen (Suppl. Figure S4C).

WB analysis showed that silmitasertib used alone or with β-estradiol did not cause any significant change in EPO-R levels, whilst the combined treatments produced a significant decrease of STAT5 and GATA1 total protein levels and a trend towards reduction in FOG1, thus mirroring the changes detected in fetal liver KO erythroid cells, except for AKT and ERK levels that remained unaffected (Figures 6C and S4E). Silmitasertib also caused a decrease of PTEN inhibitory phosphorylation (S380/T382/383) and of CK2α-dependent phosphorylation of AKT on S129 but not of phospho-GATA1 S301, phospho-AKT S473

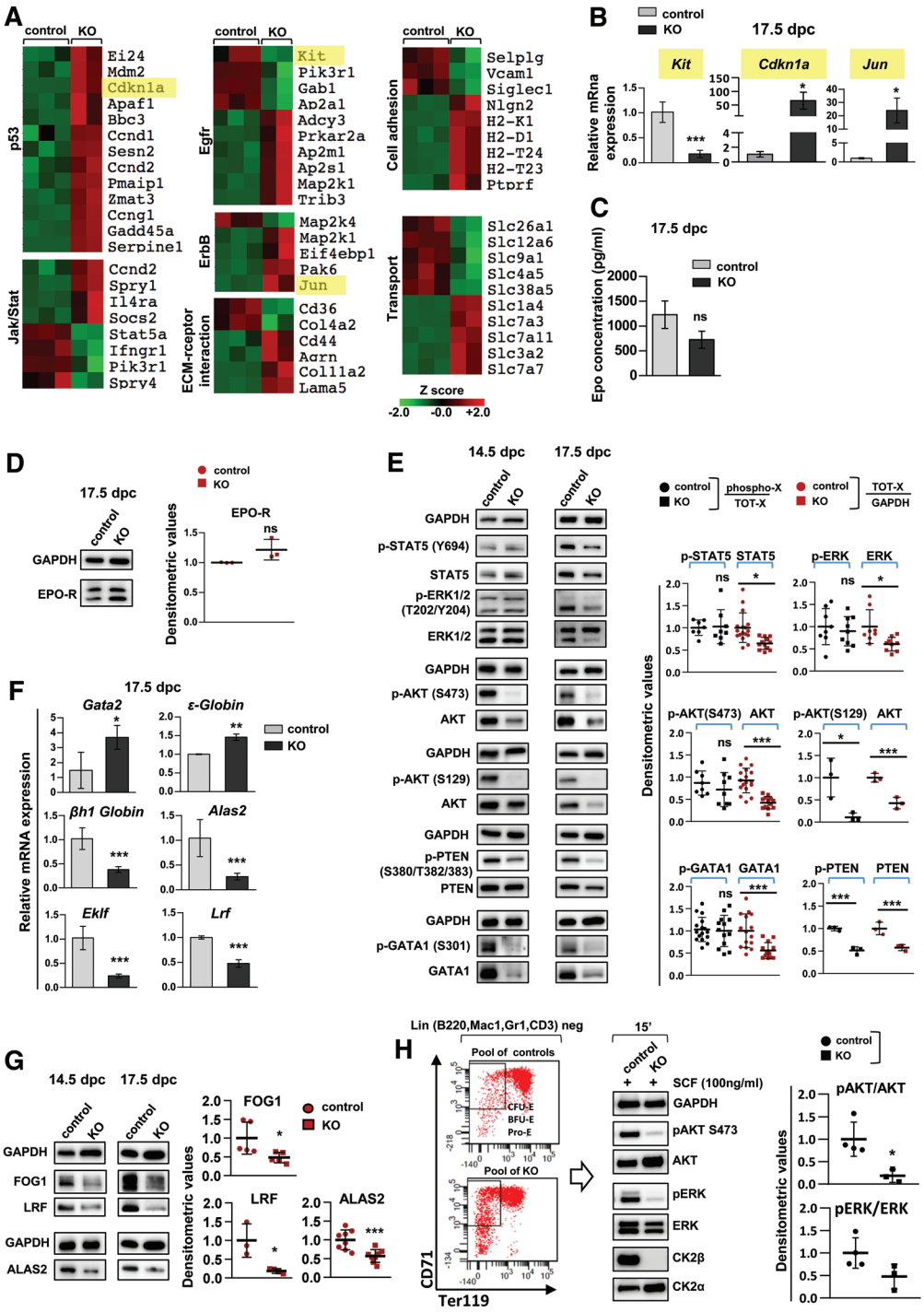

Figure 5. Lack of CK2β affects erythroid-associated signaling pathways. (A) RNA-Seq analysis on RNA extracted from sorted Ter119⁺ control and KO fetal liver cells (14.5 dpc): heat maps of the genes significantly up or down-modulated after pathway enrichment analysis. Values are quantified by the scale bar that visualizes differences in the z score (expression difference/SD) relative to the mean. (B–G) Images were produced using Ter119⁺ cells purified with beads from fetal livers. In detail: (B) qRT-PCR performed to validate the different expression of some genes of the heat maps (highlighted in yellow) (*cKit, Cdkn1a, Jun*) (n = 4 for control and KO samples). (C) Elisa test, evaluation of EPO plasma levels in 17.5 dpc embryos (controls n = 5, KO n = 3). (D) WB displaying the expression of EPO-R at 17.5 dpc; top level: representative dot plot; bottom: densitometric analysis (controls n = 3, KO n = 3); (E) WB showing the expression and activation of molecules downstream EPO-R: left panel: representative images from 14.5 and 17.5 dpc; right panel: densitometric values of 17.5 dpc sample. For total proteins, the graphs report densitometric signal normalized over GAPDH and then over the mean of values in control samples. For the phosphorylated forms, densitometric analysis reports the values as fraction of the phospho over the corresponding total protein, followed by normalization over the mean values of control samples. (F) Assessment of GATA1 transcriptional capability analyzing the expression of its targets by qRT-PCR and on other key genes involved in erythroid differentiation (n = 4 for control and KO samples) and (G) WB. (H) Evaluation by WB of ERK and AKT activation on sorted CD71⁺Ter119$^{low/-}$ populations. On the left, representative dot plot with the gating strategy for sorting; in the middle, representative WB of AKT, ERK, CK2α and CK2β expression after stimulation with SCF for 15'; on the right, graphs representing AKT and ERK activating phosphorylation: densitometric values are reported as phospho/total protein levels normalized on the mean of controls. Samples size: n = 4 pools of control samples, each one composed of 3 fetal livers, and n = 3 pools of KO, each one composed of 2 fetal livers. In (F), *Gapdh* was chosen as reference gene, (G) and (H) was used as loading control. In the graphs (B–H), data are shown as mean ± SD; statistical significance was analyzed by Student's t test: $^{*}P < 0.05$, $^{**}P < 0.01$, $^{***}P < 0.001$. AKT = serine-threonine kinase; EPO = erythropoietin; EPO-R = erythropoietin-receptor; ERK = extracellular signal-regulated kinase; KO = knockout; WB = western blot.

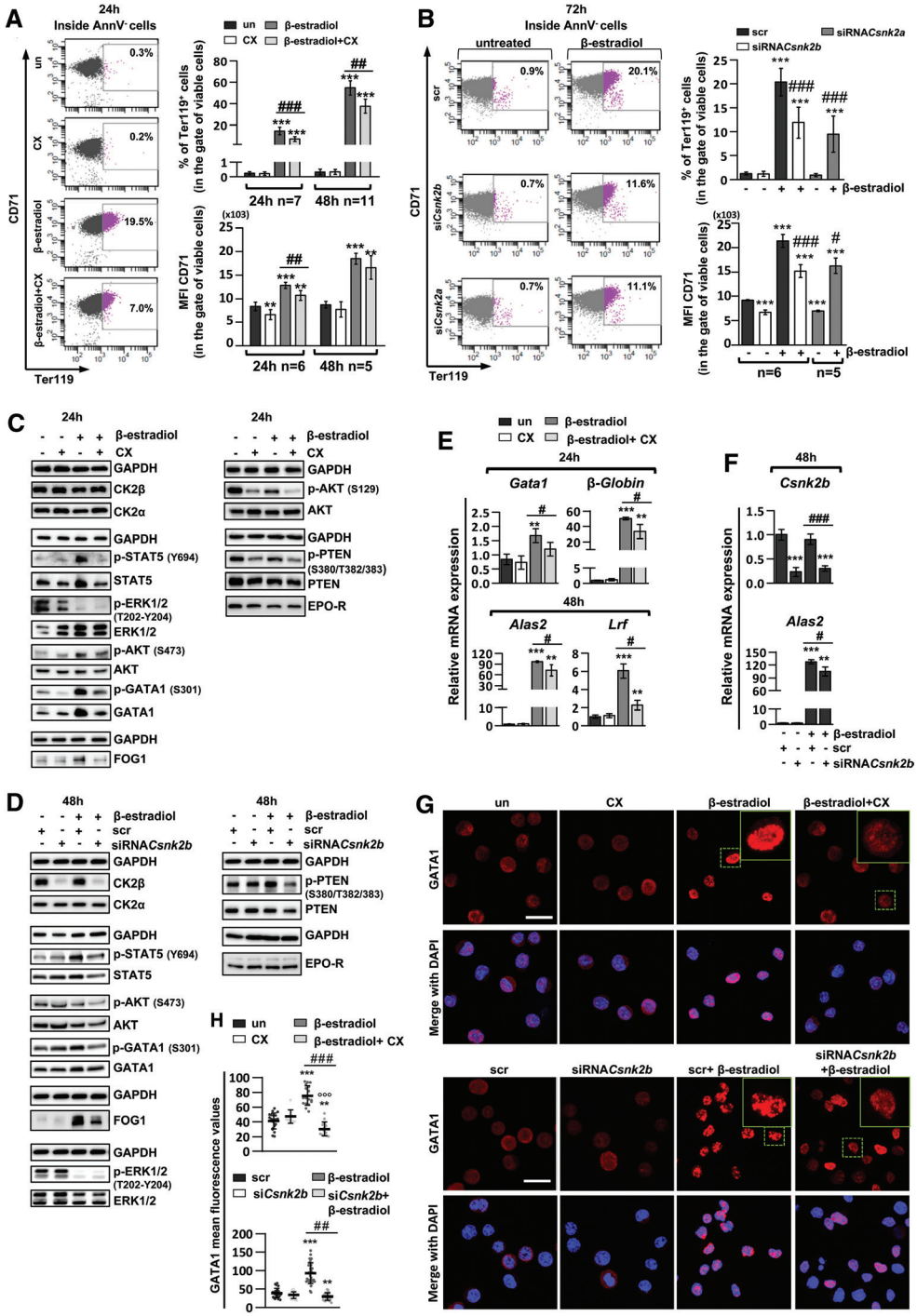

Figure 6. CK2 inhibition and *Csnk2b* knockdown impair erythroid differentiation of G1E-ER cell line through down-modulation of STAT5, GATA1, and FOG1 molecules. G1E-ER cells were induced to differentiate with β-estradiol (0.2 μM) in presence or absence of sub-apoptotic concentration of silmitasertib (CX-4945 2.5 μM). Cells were collected at 24 and 48 hours from transfection. For *Csnk2b* and *Csnk2a* down-modulation, cells were electroporated with 300pmol of siRNA or scrambled oligos, 24 hours after cells were treated with β-estradiol (0.2 μM) and collected at 48 and 72 hours. (A) Evaluation of G1E-ER differentiation upon exposure to β-estradiol and CX-4945 or (B) after *Csnk2b* or *Csnk2a* gene silencing. In both (A) and (B), on the left, representative dot plots after staining with AnnV and anti-CD71/Ter119 antibodies. The represented percentages of differentiated cells (Ter119$^+$ CD71$^+$) refer to the gate of viable cells; on the right histograms show the percentages of differentiated cells and CD71 MFI. (C) and (D) Representative WB of expression and activation of molecules downstream EPO-R upon exposure to β-estradiol and CX-4945 for 24h or (D) *Csnk2b* silencing for 48 hours (n = at least 6 independent experiments). (E) *Gata1* mRNA levels and expression of its target genes after CK2 inhibition or (F) *Csnk2b* down-modulation. GAPDH was used as loading control. (G) Immunofluorescence using anti-GATA1 antibody after treatment with CX-4945 (top panel) or *Csnk2b* siRNA (bottom panel). In red GATA1, in blue DAPI. Images were collected by confocal microscope, acquiring 10 sections along the z-stack for a total thickness of 10 μm; images are shown as maximum projection. Scale bar: 10 μm. Green squares represent higher magnification of a single cell. (H) Graphs representing GATA1 mean fluorescence intensity values of IF experiments performed in G1E-ER cells after CK2 inhibition (top panel) or *Csnk2b* siRNA (bottom panel); quantification was performed with ImageJ subtracting background signal, at least 3 images for each treatment were analyzed; each dot represents a cell. In (A), (B), and (E–H), graphs represent the mean values ± SD. Statistical significance was analyzed by Student's t-test: $^*P < 0.05$, $^{**}P < 0.01$, $^{***}P < 0.001$; *significant data compared to untreated samples; # significant data compared to β-estradiol alone; ° significant data compared to CX-4945 alone. EPO-R = erythropoietin-receptor; WB = western blot.

and phospho-ERK T202/Y204 when the phosphorylated forms were weighted on the total protein levels (Figures 6C and S4E). In the experiments of *Csnk2b* and *Csnk2a* silencing we confirmed the effective down-modulation of both subunits through WB analysis (Figures 6D and S4F); to note, it was already reported that the down-modulation of the catalytic subunit led also to a decrease of the regulatory protein[22] (Suppl. Figure S4D). *Csnk2b* silencing, even when combined with β-estradiol, did not impact on EPO-R expression, however, it caused a decline in GATA1, FOG1, STAT5, and PTEN total protein levels without significant changes in their phosphorylation sites (Figures 6D and S4F). Unlike *Csnk2b* down-modulation, *Csnk2a* silencing, when combined with β-estradiol, led only to reduction of GATA1 expression leaving unchanged FOG1 levels (Suppl. Figure S4D). Analyzing some GATA1 transcriptional targets, we discovered that silmitasertib in combination with β-estradiol, caused a drop in the mRNA expression of *β-Globin, Alas2, and Lrf/Zbtb7a* as well as of *Gata1* itself (Figure 6E), while *Csnk2b* siRNA produced effects mostly on *Alas2* gene (Figure 6F). IF showed that GATA1-ER protein accumulated exclusively in a nuclear-speckled pattern upon differentiation. Strikingly, CK2 inhibition or CK2β down-modulation, especially when combined with β-estradiol, produced a remarkable reduction in nuclear GATA1 and a redistribution in more diffuse puncta (Figure 6G). We quantified GATA1 immunofluorescence signal confirming WB results for both CK2 inhibition and *Csnk2b* silencing (Figure 6H). To test if GATA1 protein was degraded through the proteasome, we performed *Csnk2b* silencing in the presence of β-estradiol and the proteasome inhibitor bortezomib (Bz). Remarkably, WB analyses showed that Bz was effective in recovering GATA1 levels, especially upon *Csnk2b* siRNA in combination with β-estradiol (Suppl. Figure S4G). Since GATA1 degradation by proteasome is preceded by its inactivation through caspase cleavage,[74] we evaluated whether the blockade of caspases could produce similar results in GATA1 protein level restoration. As expected, the effects produced by the pan-caspase inhibitor Z-Vad-FMK[75] and silmitasertib (data not shown) instead of *Csnk2b* siRNA (Suppl. Figure S4H and S4I) were comparable to the previous ones obtained with Bz. The blockade of protein synthesis with cycloheximide in combination with β-estradiol and silmitasertib produced a higher decrease of GATA1 levels compared to cycloheximide and β-estradiol combo, indicating a faster turnover of this protein when CK2 is inhibited (Suppl. Figure S4J).

Summarizing, these data demonstrate that CK2 regulates GATA1 turnover, intracellular distribution, and transcriptional activity during erythroid differentiation.

CK2 regulates HSP70-GATA1 association

The chaperone HSP70 binds and protects GATA1 in the nucleus from the premature cleavage by caspase-3 in erythroid precursors.[76] Therefore, we evaluated HSP70 protein levels in Ter119$^+$ cells purified from fetal livers of KO and control mice. WB showed a trend in decrease of HSP70 expression in 14.5 dpc KO samples that became significant at 17.5 dpc (Figure 7A). A similar down-modulation of HSP70 protein levels was observed in G1E-ER cell line upon *Csnk2b* silencing plus β-estradiol (Figure 7B). However, the reduction of HSP70 was only at the protein level; indeed, we detected an opposite trend analyzing *Hsp70* mRNA expression in CK2β KO embryos or after its down-modulation in G1E-ER cells (Suppl. Figure S5A upper and lower panels respectively). Unlike CK2β depletion, CK2 inhibition did not produce a decrease of HSP70 protein amount (Figure 7C), prompting us to investigate the precise mechanisms of HSP70 regulation. Since HSP70 chaperoning activity is regulated by C-terminal phosphorylation mediated by CK2 and other kinases,[77] we checked HSP70 and phospho-HSP70 expression upon CK2 chemical inhibition with silmitasertib in G1E-ER cells. Unexpectedly, we did not detect any significant change in phosphorylation performing WB analysis in both total cell lysates (Figure 7C) and in the nuclear fraction (Suppl. Figure S5B). Moreover, investigation of HSP70 localization by WB in nuclear and cytoplasm extracts (Suppl. Figure S5C) as well as by IF (Suppl. Figure S5D) did not evidence significant changes in its distribution upon 24 hours of treatment with β-estradiol, CX-4945 or the combination of the 2 compounds. We next checked if CK2 inactivation could affect the GATA1/HSP70 binding by performing proximity ligation assay (PLA) (Figure 7D). HSP70-GATA1 interaction was confirmed in G1E-ER cell line in untreated condition or after β-estradiol alone. However, proximity was significantly reduced after exposure for 24 hours to silmitasertib with or without β-estradiol. Although at 24 hours the protein levels of GATA1 in the combo treatment were already reduced and could partially account for the decrease of PLA dots, the results upon single treatment with CX-4945, which did not produce changes in GATA1 expression, indicate a real decrease in GATA1/HSP70 interactions. Analysis performed at an earlier time point of 6 hours, when GATA1 protein levels are still not altered by CK2 inhibition, showed a significant reduction of PLA dots in the combo treatment when compared with untreated condition (Figure 7D).

Next, we observed in fetal liver cells of 14.5 dpc control mice, that GATA1 and CK2β displayed partial co-localization in the nuclear compartment (Figure 7E). In untreated G1E-ER cells both at 6h (Figure 7F) and 24h after plating (Suppl. Figure S5E), CK2β was distributed diffusely and partially co-localized with GATA1 in the nucleus. Co-localization persisted after β-estradiol addition with an enrichment of the signals of both proteins in the nuclei (Suppl. Figure S5E and S5F). Intriguingly, CK2 inhibition caused a redistribution of CK2β in a diffuse pattern much less overlapping with GATA1 (Figure 7F). In addition, immunofluorescence (IF) experiments showed that CK2α and β subunits co-localized in G1E-ER cells in untreated conditions and after 24 hours of β-estradiol exposure with accumulation in the nuclear compartment, thus indicating the presence of CK2 holoenzyme during erythroid differentiation (Suppl. Figure S5G). Intriguingly, silmitasertib in combination with β-estradiol produced the reduction of the nuclear amount of both α and β subunits (Suppl. Figure S5G). We also checked CK2β and HSP70 relationship. IF performed on G1E-ER cells at basal condition revealed the absence of co-localization in the nuclear compartment (Figure 7G), data confirmed also through PLA assay in this cell line and in fetal liver cells (unsorted) from control embryos (Figure 7H). Altogether, these results suggest that CK2 might control GATA1 through a dual mechanism: CK2β is involved in sustaining HSP70 protein levels, while CK2α-dependent kinase activity is important for the maintenance of HSP70-GATA1 interactions, likely independent on HSP70 phosphorylation.

A schematic molecular model of our findings is summarized in Figure 8.

DISCUSSION

We have herein described the phenotype of mice lacking CK2β in the hematopoietic compartment and provided substantial evidence of a key role of this protein in 2 processes: (1) HSPCs progression towards more differentiated precursors; (2) regulation of erythropoiesis, exerted by controlling proliferation, apoptosis and GATA1 function.

We discovered that CK2β -deficient HSCs are expanded, due to a higher proliferation rate, but at the same time an amount of these cells undergoes apoptosis (Figure 2). This is in line with our previous findings in leukemia stem cells[23] and other studies that demonstrate the importance of CK2 in sustaining cell viability and the quite different roles of the 2 CK2 subunits in the control of cell cycle: while CK2α is more associated to cell cycle progression,[78–80] free CK2β is also involved in cell cycle inhibition in particular in the regulation of the checkpoint

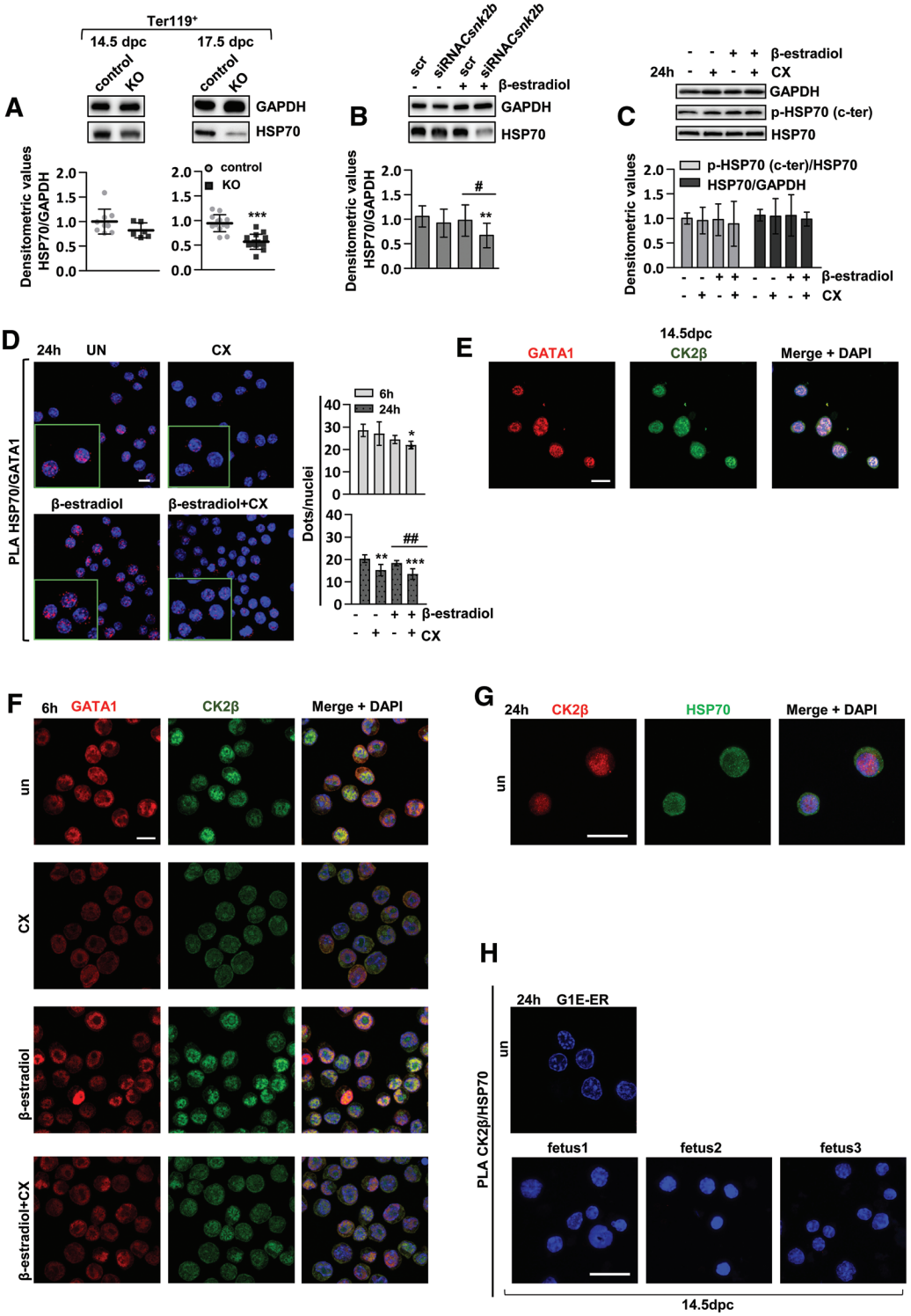

Figure 7. CK2 is involved in the control of GATA1 stability. (A) HSP70 expression by WB in Ter119+ cells purified from fetal liver at 14.5 and 17.5 dpc and (B) in G1E-ER cells upon silencing of *Csnk2b* and treatment with β-estradiol (0.2 μM). In (A) number of mice is indicated with dots (control) or squares (KO); in (B) n = 9 independent experiments. (C) Evaluation of HSP70 protein levels through WB upon CK2 inhibition with CX-4945 (2.5 μM) and induction of differentiation with β-estradiol (0.2 μM) (n = 16 independent experiments). In (A–C), GAPDH was used as loading control. (D) PLA for HSP70 and GATA1 proteins performed in G1E-ER cells after treatment with CX-4945 and β-estradiol for 6 and 24 hours. Red dots indicate interactions, in blue the nuclei; on the right; graph showing the average number of dots/nuclei ± SD. Objective 63×, zoom 1×, acquiring 10 slices along the z-stack; the represented images are the result of maximum projection. The green squares show higher magnifications. Images are representative of 3 independent experiments. (E) Immunofluorescence of GATA1 (red) and CK2β (green) in liver cells from 14.5 dpc fetuses and (F) in G1E-ER cells after treatment with CX-4945 and β-estradiol for 6 hours. In blue the nuclei. Images are represented as a single plane; scale bar: 10 μm. (G) IF for CK2β (red) and HSP70 (green) localization in untreated G1E-ER cells and (H) proximity, through PLA assay, in the same cell line (top) or in 14.5 dpc total fetal livers of control embryos (bottom). In both (G) and (H) nuclei are stained with DAPI (blue) and images are represented as maximum projection of 10 section z-stack. 63× objective, zoom 2×. Scale bar: 10μm. In (A–D), graphs represent mean ± SD. Statistical significance was analyzed by Student's t test: *$P < 0.05$, **$P < 0.01$, ***$P < 0.001$; *significant compared to untreated samples; # significant compared to β-estradiol alone. KO = knockout; PLA = proximity ligation assay; WB = western blot.

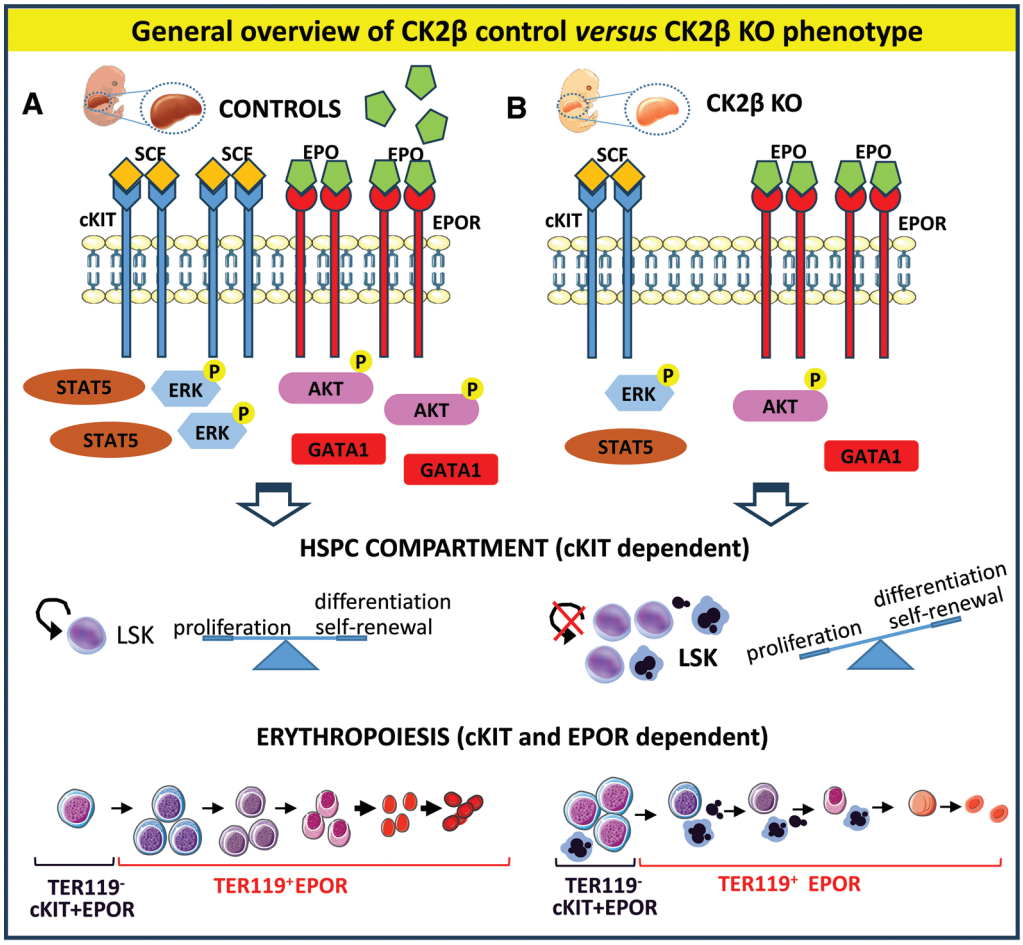

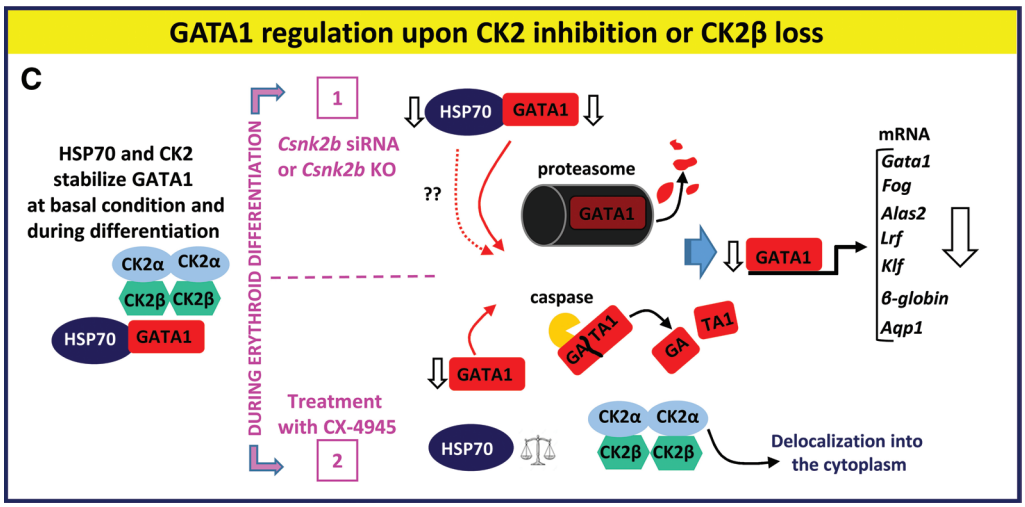

Figure 8. Visual summary of molecular changes upon CK2β KO/down-modulation or CK2 inhibition. (A) Molecular phenotype of control vs (B) CK2β KO embryos focusing on cKIT and EPO-R signaling pathways and the effects of their alterations on HSPC and erythroid cell fate. KO embryos are pale with a smaller liver, and present a lower expression of cKIT receptor but normal levels of EPO-R with reduced levels of plasma EPO; downstream both receptors in KO samples AKT and ERK effectors are less activated and reduced in total amount; there is also depletion of STAT5 and GATA1 transcription factors. Deregulation of these pathways lead to expansion of LSK population with likely a reduction in self-renewal capability, and a partial impairment of cell viability and differentiation potential. On erythroid compartment, loss of CK2β causes an accumulation of immature Ter119$^-$ erythroblasts with reduction of their proliferation rate and a partial apoptosis; in Ter119$^+$ fraction CK2β loss leads to the impairment of final differentiation with reduction of mature erythrocytes also due to increased apoptosis. Moreover, more mature erythroid cells show morphologic alterations with increased dimensions, membrane irregular shape, and less deformability. (C) Proposed model of CK2-dependent control of GATA1 stability. The dashed arrow indicates a still unknown mechanism. (1-top) lack of CK2β impairs GATA1 stability and enhances its degradation; CK2β absence causes also HSP70 protein level reduction, likely compromising its synthesis or increasing its turnover, and this event might accelerate the degradation of the transcription factor. (2-down) treatment with CX-4945 during erythroid differentiation causes delocalization of CK2 from the nuclear compartment and in turn, destabilizes HSP70/GATA1 complex. HSP70 levels are not decreased and HSP70 is not de-localized into cytoplasm after treatment with CX-4945; however, there are less interactions between the 2 proteins, making GATA1 more prone for degradation. In both conditions, 1 and 2, GATA1 turnover is increased by means of proteasome and caspase activation; the reduction of GATA1 levels leads to the decrease of its transcription activity.
AKT = serine-threonine kinase; EPO-R = erythropoietin-receptor; ERK = extracellular signal-regulated kinase; HSCs = hematopoietic stem cells; KO = knockout.

between G2/M phases.[81,82] Moreover, HSPCs exhibited alterations in the expression of transcription factors important for the maintenance of stemness properties as well as for lineage commitment[40,42,44,46,47] (Figure 2H). Thus, a combination of different problems such as the unbalanced expression of these factors, the higher mitotic rate, and reduced cell viability could lead to the loss of quiescence and subsequent exhaustion of HSPC pools coupled with reduction of their differentiation potential. Altogether, these several elements would also explain, at least in part, the impairment of HSPC engraftment in competitive (Figure 3) and non-competitive (Suppl. Figure S1C-E) transplantation experiments and the reduced capability to form colonies in a selective environment such as in methylcellulose cultures (Suppl. Figure S1A and S1B). Although we did not observe a reduction in CXCR4 expression in CK2β KO HSPCs (Fig. 3G), we do not completely exclude reduced capabilities in homing process to the BM of these cells. Moreover, alteration in transcription factors could favor the commitment towards preferred populations such as monocyte/macrophages and granulocytes observed in KO embryos. Thus, these data suggest that CK2β might tune the HSPCs' balance between proliferation and differentiation. FACS analysis pointed out that CK2β KO embryos were able to produce some mature hematopoietic cells (Figure 1) of the myeloid lineage that likely undergo apoptosis at later time points. Thus, a combination of alterations in cell viability and in differentiation programs could determine the CK2β KO phenotype such as the reduced cellularity of fetal livers. To note, KO embryos also displayed reduction in B mature ($B220^+CD19^+$) cells with expansion in percentages of immature pre/pro B population, data that support our previous finding obtained in the *Csnk2b*$^{fl/fl}$/*CD19*$^{+/Cre}$ KO mouse model.[35] The depletion of mature erythroid compartment ($Ter119^+$) in CK2β KO embryos is another cause of reduced fetal liver cellularity. We discovered stage-dependent erythroid functions for CK2β. CK2β promotes cell cycle progression in immature erythroblasts ($Ter119^-CD71^+$) protects from apoptosis and supports differentiation in mature $Ter119^+$ cells.

The significant reduction of cKit expression in KO samples might contribute to the observed alterations in HSPCs and erythroblasts (Figures 2F and 4C). Indeed, at the BFU-E stage, cells are mainly dependent on cKit receptor for proliferation and differentiation,[83] while in CFU-E and in pro-erythroblasts stages cKit is co-expressed with EPO-R and is able to transactivate EPO-R intracellular domain.[3,58,83] We demonstrated that in $Ter119^{-/low}CD71^+$ population sorted from CK2β KO fetal livers, which contains CFU-E, BFU-E, and pro-E, the key downstream effectors, such as ERK and AKT, are less activated (Fig. 5H). Thus, it is conceivable that an impairment of cKit and EPO-R signaling accounts for the proliferative and differentiation defects. Although in CK2β KO more mature erythroid cells ($Ter119^+$) we did not detect a depletion in EPO-R protein levels (Figure 5D), the trend of reduction in EPO concentration could suggest a less effective stimulation upstream of this receptor (Figure 5C). Since during fetal life EPO is mainly produced by hepatocytes and macrophages of the blood islands,[84] we cannot exclude that macrophage production of EPO is impaired in CK2β KO embryos. Moreover, we observed in KO embryos the down-modulation of *Siglec1*, *Vacam1,* and *Selplg* (Figure 5A) encoding for the adhesion molecules essential for the blood island formation.[61] These data may suggest that there are looser interactions between nurse macrophages and erythroblast cells with potential negative impact on erythroid maturation and viability. Biochemical and RNA-seq experiments confirmed the ineffective activation of cKit and EPO-R downstream cascades (Figure 5A and 5E). For instance, CK2β was found important to positively regulate STAT5 (Figure 5A and 5E) that has a key role in EPO-dependent erythropoiesis being mainly involved in the up-regulation of BCL-xL expression.[85,86] The inhibitory effect on BCL-XL seems to be specific to this BCL-2 family member; indeed, focusing on other factors belonging to the same protein family, we observed an increase of the anti-apoptotic factor MCL-1 in $Ter119^+$ CK2β KO samples, likely due to an (ineffective) attempt to sustain cell viability. While BCL-XL is a key survival factor in more mature erythroid cells, MCL-1 is reported to be more important for erythroid precursors.[57] $Ter119^+$ cells from CK2β-null samples evidenced also the up-regulation of the pro-apoptotic proteins BAX and PUMA, showing overall a clear unbalance versus cell death signals. We discovered that CK2β sustains 2 other key erythroid transcription factors, GATA1 and FOG1, whose reduction in KO samples was associated to the consequential down-modulation of *Lrf*, *Klf*, *β-Globin, and Alas2* target genes. To further support our data, in particular the impairment of β-Globin production, Ouyang et al[87] demonstrated that CK2 is involved in the positive regulation of EKLF transcriptional activity through direct phosphorylation of its interaction domain. Altogether, this transcriptional dysfunction might underlie the phenotypic changes of higher apoptosis, accumulation of immature erythroblasts, presence of non-heme iron deposits (Suppl. Figure S3F), and abnormal shape likely due to deregulation of adhesion molecules and ion/water-channels as suggested by alteration of *Aqp1* and *Slc* gene expression.[63] Moreover, we confirmed through ektacytometer analysis less deformability of CK2β KO erythrocytes (Figure 4G), underlying a higher risk of hemolysis when these cells are exposed to mechanical stresses in the blood stream.

In CK2β KO mice the effect on erythroid lineage is likely due to both lack of β chains and a decrease of CK2 enzymatic activity; depletion of β subunits inhibits holoenzyme formation, thus partially impinging on kinase efficiency, but it might also make the α subunits more unstable and be degraded as suggested by the reduction of CK2α protein levels in CK2β-null $Ter119^+$ cells (Figure 4A). Heterozygous mice are not anemic although adult animals present some alterations in bone marrow and spleen; this mild phenotype could be explained since β subunits are produced in large excess compared to catalytic counterparts,[12] thus the half-dose of CK2β is likely sufficient to keep CK2 kinase activity at normal levels (Suppl. Figure S2B) and to preserve CK2β independent functions without reducing cell viability or influencing dramatically erythroid differentiation.

The dysfunctional GATA1/FOG1 activity, by impinging on platelet formation, could also explain the presence of hemorrhages in KO embryos (Figure 1A). Indeed, aberrant platelet development and function have been recently demonstrated in the conditional CK2β$^{fl/fl}$PF4-Cre mouse model in megakaryocytes.[88] We can suppose that the ineffective hemostasis in the CK2β KO embryos might concur with the impaired erythropoiesis to premature lethality. Moreover, given the broad functions of this kinase, it is conceivable that the erythroid phenotype in KO mice could be the result of the simultaneous impairment of other transcription factors (*Ikzf1, Klf13, Smad3*) as indicated by RNA-seq data (Figures 5 and S3B, S3C).[64,65,89]

We have provided substantial evidence that CK2 could control GATA1 mainly through post-translational mechanisms. To note, RNA-seq results suggest a widespread control by CK2β of genes that encode for ubiquitin ligases (*Trim*[90] and *Rnf*[91] family genes) and deubiquitinases (*Usp* genes) (Suppl. Tables S1 and S2). Thus, the extensive signaling impairment downstream EPO-R could be linked to a shared CK2β-regulated mechanism, whereby this protein would be essential to avoid an excessively fast protein turnover. To suggest such a possible mechanism, we exploited G1E-ER cell model of erythroid differentiation. We confirmed in these cells, upon CK2 inhibition or *Csnk2b* silencing and induction of differentiation, the molecular alterations obtained in vivo for the signal cascades downstream EPO-R. However, some discrepancies in the results obtained between the in vivo and in vitro systems could be due to the lack of terminal erythroid differentiation capability of G1E-ER cells[6,71–73]

and the residual expression of CK2β in silencing experiments. Moreover, some differences between CK2 inhibitor and *Csnk2b* silencing effects are reasonable considering that the free amount of β dimers[12] could still work as chaperone when the alpha kinase activity is inhibited. With this cell line model, we partially elucidated the molecular mechanisms of CK2-dependent GATA1 regulation: CK2 maintains the nuclear localization and distribution of GATA1 and upholds its levels, likely by potentiating the activity of HSP70, which is central in regulating GATA1 protein degradation rate preventing its cleavage by caspases.[76] CK2β sustains HSP70 levels in erythroid cells through a mechanism independent from the phosphorylation of the C-terminal region (Figure 7C), known to contain target residues of CK2, CK1, and GSK3 kinases.[77] Evidence suggests that while CK2β might keep high the levels of HSP70, CK2α might regulate the stability of the HSP70- GATA1 association (Figure 7D). Although CK2 co-localizes with GATA1 in the nuclear compartment at basal condition and during differentiation (Figures 7E, 7F, and S5E), the exact mechanism exploited by CK2 to control HSP70 abundance, thus influencing GATA1 stability, has not been elucidated yet. Considering the lack of co-localization in IF and signal in PLA assays performed with CK2β and HSP70 probes (Figure 7G and 7H), a direct interaction between these 2 proteins is unlikely.

Also, HSP70 abundance may not be essential in the CK2-mediated stabilization of GATA1 at mid-gestation, since the reduction of GATA1 in fetal liver KO Ter119$^+$ cells occurred earlier (14.5 dpc) than that of HSP70 (17.5 dpc) (Figures 5E and 7A). We demonstrated that inhibition of caspases with ZVAD (Suppl. Figures S4H and S4I) or blockade of proteasomes, through bortezomib (Suppl. Figure S4G), can rescue GATA1 nuclear expression upon CK2β down-modulation or CK2 chemical inhibition. These data indicate that in our experimental conditions, both mechanisms are involved in GATA1 degradation. Caspase activity seems to be more linked to CK2-dependent regulation of HSP70, whereas degradation through proteasome might be driven by other mechanisms that have not been elucidated yet: (1) CK2-dependent control of ubiquitin ligases or deubiquitinases, as suggested by RNA-seq data, or (2) CK2 possible influence on other axis of degradation such as the one mediated by phosphorylation and acetylation of GATA1 followed by its interaction with co-chaperone Hsp27.[92] Moreover, the kinase activity was found to be required to keep CK2β and CK2α in the nucleus closer to the GATA1/HSP70 complex (Figures 7F and S5D) but it does not seem to influence HSP70 intracellular localization (Suppl. Figures S5C and S5D). To this regard, Filhol O. et al.[93] postulated that nuclear localization may sustain the function of CK2 and it is known that CK2β autophosphorylation on Ser2 and Ser3 relies on to the formation of a CK2 multimeric structure[94] that in turn might reduce the nuclear-cytoplasmic shuttling of the kinase. It has also been reported that autophosphorylation on Ser2, Ser3, and that on Ser209 (this latter indirectly mediated by CK2 through the intermediate effector CDK1 kinase) could be important in the regulation of CK2β degradation.[95,96] Thus, the loss of CK2 might affect GATA1 levels in 2 sequential steps: (1) upon the reduction of CK2β and of CK2α kinase activity an increased rate of GATA1 degradation occurs when differentiation is induced; (2) the subsequent dissociation of the HSP70-GATA1 complex or depletion of HSP70 causes a further degradation of the transcription factor. Since CK2α and CK2β could also work independently from each other, we can hypothesize that they might influence HSP70 in different ways, one playing on HSP70 levels and the other one on HSP70 ability to interact with other proteins.

In conclusion, the described novel functions for CK2β in HSPC biology and erythropoiesis and in the EPO-R and GATA1 signaling, indicate a key role for this kinase as a master regulator of blood cell development.

ACKNOWLEDGMENTS

Prof. Mitchell J. Weiss (St. Jude Children's Research Hospital, USA) for providing us G1E-ER cell line; Prof. B. Vojtesek (Masaryk Memorial Cancer Institute from Czech Republic) for the p-HSP70 antibody; Dr. Anna Cabrelle (Veneto Institute of Molecular Medicine—VIMM) for helping with sorting experiments by FACS; Dr. Vito Barbieri, Dr. Ilaria Marigo and Prof. Antonio Rosato (Istituo Oncologico Veneto-IOV- Padova) for breeding and irradiation of CD45.1 mice.

AUTHOR CONTRIBUTIONS

LQT performed research, analyzed data, and wrote the manuscript; SNC and EM helped with flow cytometry and manuscript revision; EDB and AF helped with mice genotyping and flow cytometry; MP, MN, and CG contributed to the morphological analysis of tissues and cells; NV analyzed the RNA-Seq data; MD, RC, MM, and MPB performed and helped in deformability assay; MA helped in mice transplantation; SM, ZS, and GPF helped in manuscript editing; OF and BB provided the transgenic mice; GS, LT, SM, and FV provided funding and/or helped in the revision of the manuscript; FP conceived and designed the study, provided funding, supervised research and data analysis and wrote/edited the manuscript.

DISCLOSURES

The authors have no conflicts of interest to disclose

SOURCES OF FUNDING

This work was supported by Grants from the Italian Ministry of Education, University and Research (FIRB—Futuro in Ricerca n. RBFR086EW9_001); the Associazione Italiana per la Ricerca sul Cancro (AIRC) (n.14481 and 18387 to FP; #15286 to GS; #2524 to LT); the University of Padova (Progetti di Ricerca di Ateneo n.CPDA114940/11) to FP, PRIN (Progetti di rilevante interesse nazionale)-MIUR Prot.2017ZXT5WR to SM.

DATA AND MATERIALS AVAILABILITY

As indicated in the Material and Methods the complete RNA-Seq data are available in the Gene Expression Omnibus (GEO) (http://www.ncbi.nlm.nih.gov/geo) under accession number GSE158665. All the other data are available in the main text or the supplementary materials.

REFERENCES

1. Bonavita O, Mollica Poeta V, Massara M, et al. Regulation of hematopoiesis by the chemokine system. *Cytokine*. 2018;109:76–80.
2. Keller G, Lacaud G, Robertson S. Development of the hematopoietic system in the mouse. *Exp Hematol*. 1999;27:777–787.
3. Munugalavadla V, Kapur R. Role of c-kit and erythropoietin receptor in erythropoiesis. *Crit Rev Oncol Hematol*. 2005;54:63–75.
4. Chateauvieux S, Grigorakaki C, Morceau F, et al. Erythropoietin, erythropoiesis and beyond. *Biochem Pharmacol*. 2011;82:1291–1303.
5. Ferreira R, Ohneda K, Yamamoto M, et al. GATA1 function, a paradigm for transcription factors in hematopoiesis. *Mol Cell Biol*. 2005;25:1215–1227.
6. Gregory T, Yu C, Ma A, et al. GATA-1 and erythropoietin cooperate to promote erythroid cell survival by regulating bcl-xL expression. *Blood*. 1999;94:87–96.
7. Maeda T, Ito K, Merghoub T, et al. LRF is an essential downstream target of GATA1 in erythroid development and regulates BIM-dependent apoptosis. *Dev Cell*. 2009;17:527–540.
8. Sankaran VG, Xu J, Orkin SH. Advances in the understanding of haemoglobin switching. *Br J Haematol*. 2010;149:181–194.
9. Zhang Y, Zhang J, An W, et al. Intron 1 GATA site enhances ALAS2 expression indispensably during erythroid differentiation. *Nucleic Acids Res*. 2017;45:657–671.
10. Chiba T, Ikawa Y, Todokoro K. GATA-1 transactivates erythropoietin receptor gene, and erythropoietin receptor-mediated signals enhance GATA-1 gene expression. *Nucleic Acids Res*. 1991;19:3843–3848.
11. Litchfield DW, Bosc DG, Canton DA, et al. Functional specialization of CK2 isoforms and characterization of isoform-specific binding partners. *Mol Cell Biochem*. 2001;227:21–29.
12. Bibby AC, Litchfield DW. The multiple personalities of the regulatory subunit of protein kinase CK2: CK2 dependent and CK2 independent roles reveal a secret identity for CK2beta. *Int J Biol Sci*. 2005;1:67–79.

13. Grein S, Raymond K, Cochet C, et al. Searching interaction partners of protein kinase CK2beta subunit by two-hybrid screening. *Mol Cell Biochem*. 1999;191:105–109.
14. St-Denis NA, Litchfield DW. Protein kinase CK2 in health and disease: From birth to death: the role of protein kinase CK2 in the regulation of cell proliferation and survival. *Cell Mol Life Sci*. 2009;66:1817–1829.
15. Ahmad KA, Wang G, Unger G, et al. Protein kinase CK2--a key suppressor of apoptosis. *Adv Enzyme Regul*. 2008;48:179–187.
16. Desagher S, Osen-Sand A, Montessuit S, et al. Phosphorylation of bid by casein kinases I and II regulates its cleavage by caspase 8. *Mol Cell*. 2001;8:601–611.
17. Wang D, Westerheide SD, Hanson JL, et al. Tumor necrosis factor alpha-induced phosphorylation of RelA/p65 on Ser529 is controlled by casein kinase II. *J Biol Chem*. 2000;275:32592–32597.
18. Tsuchiya Y, Asano T, Nakayama K, et al. Nuclear IKKbeta is an adaptor protein for IkappaBalpha ubiquitination and degradation in UV-induced NF-kappaB activation. *Mol Cell*. 2010;39:570–582.
19. Torres J, Pulido R. The tumor suppressor PTEN is phosphorylated by the protein kinase CK2 at its C terminus implications for PTEN stability to proteasome-mediated degradation. *J Biol Chem*. 2001;276:993–998.
20. Di Maira G, Brustolon F, Pinna LA, et al. Dephosphorylation and inactivation of Akt/PKB is counteracted by protein kinase CK2 in HEK 293T cells. *Cell Mol Life Sci*. 2009;66:3363–3373.
21. Alcaraz E, Vilardell J, Borgo C, et al. Effects of CK2beta subunit down-regulation on Akt signalling in HK-2 renal cells. *PLoS One*. 2020;15:e0227340.
22. Quotti Tubi L, Gurrieri C, Brancalion A, et al. Inhibition of protein kinase CK2 with the clinical-grade small ATP-competitive compound CX-4945 or by RNA interference unveils its role in acute myeloid leukemia cell survival, p53-dependent apoptosis and daunorubicin-induced cytotoxicity. *J Hematol Oncol*. 2013;6:78.
23. Quotti Tubi L, Canovas Nunes S, Brancalion A, et al. Protein kinase CK2 regulates AKT, NF-kappaB and STAT3 activation, stem cell viability and proliferation in acute myeloid leukemia. *Leukemia*. 2017;31:292–300.
24. Manni S, Toscani D, Mandato E, et al. Bone marrow stromal cell-fueled multiple myeloma growth and osteoclastogenesis are sustained by protein kinase CK2. *Leukemia*. 2014;28:2094–2097.
25. Manni S, Carrino M, Piazza F. Role of protein kinases CK1alpha and CK2 in multiple myeloma: regulation of pivotal survival and stress-managing pathways. *J Hematol Oncol*. 2017;10:157.
26. Manni S, Carrino M, Semenzato G, et al. Old and young actors playing novel roles in the drama of multiple myeloma bone marrow microenvironment dependent drug resistance. *Int J Mol Sci*. 2018;19:1512.
27. Mandato E, Nunes SC, Zaffino F, et al. CX-4945, a selective inhibitor of casein kinase 2, synergizes with B cell receptor signaling inhibitors in inducing diffuse large B cell lymphoma cell death. *Curr Cancer Drug Targets*. 2018;18:608–616.
28. Piazza F, Manni S, Arjomand A, et al. New responsibilities for aged kinases in B-lymphomas. *Hematol Oncol*. 2020;38:3–11.
29. Pizzi M, Piazza F, Agostinelli C, et al. Protein kinase CK2 is widely expressed in follicular, Burkitt and diffuse large B-cell lymphomas and propels malignant B-cell growth. *Oncotarget*. 2015;6:6544–6552.
30. Mandato E, Manni S, Zaffino F, et al. Targeting CK2-driven non-oncogene addiction in B-cell tumors. *Oncogene*. 2016;35:6045–6052.
31. Dominguez I, Sonenshein GE, Seldin DC. Protein kinase CK2 in health and disease: CK2 and its role in Wnt and NF-kappaB signaling: linking development and cancer. *Cell Mol Life Sci*. 2009;66:1850–1857.
32. Gotz C, Montenarh M. Protein kinase CK2 in development and differentiation. *Biomed Rep*. 2017;6:127–133.
33. Blond O, Jensen HH, Buchou T, et al. Knocking out the regulatory beta subunit of protein kinase CK2 in mice: gene dosage effects in ES cells and embryos. *Mol Cell Biochem*. 2005;274:31–37.
34. Buchou T, Vernet M, Blond O, et al. Disruption of the regulatory beta subunit of protein kinase CK2 in mice leads to a cell-autonomous defect and early embryonic lethality. *Mol Cell Biol*. 2003;23:908–915.
35. Quotti Tubi L, Mandato E, Canovas Nunes S, et al. CK2beta-regulated signaling controls B cell differentiation and function. *Front Immunol*. 2022;13:959138.
36. Weiss MJ, Yu C, Orkin SH. Erythroid-cell-specific properties of transcription factor GATA-1 revealed by phenotypic rescue of a gene-targeted cell line. *Mol Cell Biol*. 1997;17:1642–1651.
37. Medvinsky A, Rybtsov S, Taoudi S. Embryonic origin of the adult hematopoietic system: advances and questions. *Development*. 2011;138:1017–1031.
38. Yilmaz OH, Kiel MJ, Morrison SJ. SLAM family markers are conserved among hematopoietic stem cells from old and reconstituted mice and markedly increase their purity. *Blood*. 2006;107:924–930.
39. Katsumoto T, Aikawa Y, Iwama A, et al. MOZ is essential for maintenance of hematopoietic stem cells. *Genes Dev*. 2006;20:1321–1330.
40. Monteiro R, Pouget C, Patient R. The GATA1/PU1 lineage fate paradigm varies between blood populations and is modulated by tif1gamma. *EMBO J*. 2011;30:1093–1103.
41. Elagib KE, Xiao M, Hussaini IM, et al. Jun blockade of erythropoiesis: role for repression of GATA-1 by HERP2. *Mol Cell Biol*. 2004;24:7779–7794.
42. Lacombe J, Herblot S, Rojas-Sutterlin S, et al. Scl regulates the quiescence and the long-term competence of hematopoietic stem cells. *Blood*. 2010;115:792–803.
43. Park IK, Qian D, Kiel M, et al. Bmi-1 is required for maintenance of adult self-renewing haematopoietic stem cells. *Nature*. 2003;423:302–305.
44. Jacob B, Osato M, Yamashita N, et al. Stem cell exhaustion due to Runx1 deficiency is prevented by Evi5 activation in leukemogenesis. *Blood*. 2010;115:1610–1620.
45. Yokomizo T, Hasegawa K, Ishitobi H, et al. Runx1 is involved in primitive erythropoiesis in the mouse. *Blood*. 2008;111:4075–4080.
46. Iwasaki H, Somoza C, Shigematsu H, et al. Distinctive and indispensable roles of PU1 in maintenance of hematopoietic stem cells and their differentiation. *Blood*. 2005;106:1590–1600.
47. Hasemann MS, Lauridsen FK, Waage J, et al. C/EBPalpha is required for long-term self-renewal and lineage priming of hematopoietic stem cells and for the maintenance of epigenetic configurations in multipotent progenitors. *PLoS Genet*. 2014;10:e1004079.
48. Tipping AJ, Pina C, Castor A, et al. High GATA-2 expression inhibits human hematopoietic stem and progenitor cell function by effects on cell cycle. *Blood*. 2009;113:2661–2672.
49. Kwarteng EO, Heinonen KM. Competitive transplants to evaluate hematopoietic stem cell fitness. *J Vis Exp*. 2016;114:54345.
50. Gudmundsson KO, Stull SW, Keller JR. Transplantation of mouse fetal liver cells for analyzing the function of hematopoietic stem and progenitor cells. *Methods Mol Biol*. 2012;879:123–133.
51. Oguro H, Ding L, Morrison SJ. SLAM family markers resolve functionally distinct subpopulations of hematopoietic stem cells and multipotent progenitors. *Cell Stem Cell*. 2013;13:102–116.
52. Wright DE, Bowman EP, Wagers AJ, et al. Hematopoietic stem cells are uniquely selective in their migratory response to chemokines. *J Exp Med*. 2002;195:1145–1154.
53. Koulnis M, Pop R, Porpiglia E, et al. Identification and analysis of mouse erythroid progenitors using the CD71/TER119 flow-cytometric assay. *J Vis Exp*. 2011;54:2809.
54. Zhang J, Socolovsky M, Gross AW, et al. Role of RAS signaling in erythroid differentiation of mouse fetal liver cells: functional analysis by a flow cytometry-based novel culture system. *Blood*. 2003;102:3938–3946.
55. Boles NC, Peddibhotla S, Chen AJ, et al. Chk1 haploinsufficiency results in anemia and defective erythropoiesis. *PLoS One*. 2010;5:e8581.
56. Yang F, Huang Y, Chen X, et al. Deletion of a flippase subunit Tmem30a in hematopoietic cells impairs mouse fetal liver erythropoiesis. *Haematologica*. 2019;104:1984–1994.
57. Turnis ME, Kaminska E, Smith KH, et al. Requirement for antiapoptotic MCL-1 during early erythropoiesis. *Blood*. 2021;137:1945–1958.
58. Kapur R, Zhang L. A novel mechanism of cooperation between c-Kit and erythropoietin receptor Stem cell factor induces the expression of Stat5 and erythropoietin receptor, resulting in efficient proliferation and survival by erythropoietin. *J Biol Chem*. 2001;276:1099–1106.
59. Peng HY, Jiang SS, Hsiao JR, et al. IL-8 induces miR-424-5p expression and modulates SOCS2/STAT5 signaling pathway in oral squamous cell carcinoma. *Mol Oncol*. 2016;10:895–909.
60. Zwifelhofer NM, Cai X, Liao R, et al. GATA factor-regulated solute carrier ensemble reveals a nucleoside transporter-dependent differentiation mechanism. *PLoS Genet*. 2020;16:e1009286.
61. Jacobsen RN, Perkins AC, Levesque JP. Macrophages and regulation of erythropoiesis. *Curr Opin Hematol*. 2015;22:212–219.
62. Millard SM, Heng O, Opperman KS, et al. Fragmentation of tissue-resident macrophages during isolation confounds analysis of single-cell preparations from mouse hematopoietic tissues. *Cell Rep*. 2021;37:110058.
63. Hasegawa A, Shimizu R, Mohandas N, et al. Mature erythrocyte membrane homeostasis is compromised by loss of the GATA1-FOG1 interaction. *Blood*. 2012;119:2615–2623.
64. Bottardi S, Ross J, Bourgoin V, et al. Ikaros and GATA-1 combinatorial effect is required for silencing of human gamma-globin genes. *Mol Cell Biol*. 2009;29:1526–1537.
65. Gordon AR, Outram SV, Keramatipour M, et al. Splenomegaly and modified erythropoiesis in KLF13-/- mice. *J Biol Chem*. 2008;283:11897–11904.

66. Zhao W, Kitidis C, Fleming MD, et al. Erythropoietin stimulates phosphorylation and activation of GATA-1 via the PI3-kinase/AKT signaling pathway. *Blood*. 2006;107:907–915.
67. Di Maira G, Salvi M, Arrigoni G, et al. Protein kinase CK2 phosphorylates and upregulates Akt/PKB. *Cell Death Differ*. 2005;12:668–677.
68. Tsang AP, Visvader JE, Turner CA, et al. FOG, a multitype zinc finger protein, acts as a cofactor for transcription factor GATA-1 in erythroid and megakaryocytic differentiation. *Cell*. 1997;90:109–119.
69. Harigae H, Nakajima O, Suwabe N, et al. Aberrant iron accumulation and oxidized status of erythroid-specific delta-aminolevulinate synthase (ALAS2)-deficient definitive erythroblasts. *Blood*. 2003;101:1188–1193.
70. Siddiqui-Jain A, Drygin D, Streiner N, et al. CX-4945, an orally bioavailable selective inhibitor of protein kinase CK2, inhibits prosurvival and angiogenic signaling and exhibits antitumor efficacy. *Cancer Res*. 2010;70:10288–10298.
71. Jain D, Mishra T, Giardine BM, et al. Dynamics of GATA1 binding and expression response in a GATA1-induced erythroid differentiation system. *Genom Data*. 2015;4:1–7.
72. Welch JJ, Watts JA, Vakoc CR, et al. Global regulation of erythroid gene expression by transcription factor GATA-1. *Blood*. 2004;104:3136–3147.
73. Rylski M, Welch JJ, Chen YY, et al. GATA-1-mediated proliferation arrest during erythroid maturation. *Mol Cell Biol*. 2003;23:5031–5042.
74. Solier S, Fontenay M, Vainchenker W, et al. Non-apoptotic functions of caspases in myeloid cell differentiation. *Cell Death Differ*. 2017;24:1337–1347.
75. Zermati Y, Garrido C, Amsellem S, et al. Caspase activation is required for terminal erythroid differentiation. *J Exp Med*. 2001;193:247–254.
76. Ribeil JA, Zermati Y, Vandekerckhove J, et al. Hsp70 regulates erythropoiesis by preventing caspase-3-mediated cleavage of GATA-1. *Nature*. 2007;445:102–105.
77. Muller P, Ruckova E, Halada P, et al. C-terminal phosphorylation of Hsp70 and Hsp90 regulates alternate binding to co-chaperones CHIP and HOP to determine cellular protein folding/degradation balances. *Oncogene*. 2013;32:3101–3110.
78. Homma MK, Homma Y. Regulatory role of CK2 during the progression of cell cycle. *Mol Cell Biochem*. 2005;274:47–52.
79. Litchfield DW. Protein kinase CK2: structure, regulation and role in cellular decisions of life and death. *Biochem J*. 2003;369:1–15.
80. Theis-Febvre N, Filhol O, Froment C, et al. Protein kinase CK2 regulates CDC25B phosphatase activity. *Oncogene*. 2003;22:220–232.
81. Guerra B, Issinger OG, Wang JY. Modulation of human checkpoint kinase Chk1 by the regulatory beta-subunit of protein kinase CK2. *Oncogene*. 2003;22:4933–4942.
82. Kreutzer J, Guerra B. The regulatory beta-subunit of protein kinase CK2 accelerates the degradation of CDC25A phosphatase through the checkpoint kinase Chk1. *Int J Oncol*. 2007;31:1251–1259.
83. Wu H, Liu X, Jaenisch R, et al. Generation of committed erythroid BFU-E and CFU-E progenitors does not require erythropoietin or the erythropoietin receptor. *Cell*. 1995;83:59–67.
84. Zucali JR, Stevens V, Mirand EA. In vitro production of erythropoietin by mouse fetal liver. *Blood*. 1975;46:85–90.
85. Watowich SS, Mikami A, Busche RA, et al. Erythropoietin receptors that signal through Stat5 or Stat3 support fetal liver and adult erythropoiesis: Lack of specificity of stat signals during red blood cell development. *J Interferon Cytokine Res*. 2000;20:1065–1070.
86. Gillinder KR, Tuckey H, Bell CC, et al. Direct targets of pSTAT5 signalling in erythropoiesis. *PLoS One*. 2017;12:e0180922.
87. Ouyang L, Chen X, Bieker JJ. Regulation of erythroid Kruppel-like factor (EKLF) transcriptional activity by phosphorylation of a protein kinase casein kinase II site within its interaction domain. *J Biol Chem*. 1998;273:23019–23025.
88. Münzer P, Walker-Allgaier B, Geue S, et al. CK2β regulates thrombopoiesis and Ca^{2+}-triggered platelet activation in arterial thrombosis. *Blood*. 2017;130:2774–2785.
89. Adelman CA, Chattopadhyay S, Bieker JJ. The BMP/BMPR/Smad pathway directs expression of the erythroid-specific EKLF and GATA1 transcription factors during embryoid body differentiation in serum-free media. *Development*. 2002;129:539–549.
90. Crawford LJ, Johnston CK, Irvine AE. TRIM proteins in blood cancers. *J Cell Commun Signal*. 2018;12:21–29.
91. Joazeiro CA, Weissman AM. RING finger proteins: mediators of ubiquitin ligase activity. *Cell*. 2000;102:549–552.
92. de Thonel A, Vandekerckhove J, Lanneau D, et al. HSP27 controls GATA-1 protein level during erythroid cell differentiation. *Blood*. 2010;116:85–96.
93. Filhol O, Nueda A, Martel V, et al. Live-cell fluorescence imaging reveals the dynamics of protein kinase CK2 individual subunits. *Mol Cell Biol*. 2003;23:975–987.
94. Pagano MA, Sarno S, Poletto G, et al. Autophosphorylation at the regulatory beta subunit reflects the supramolecular organization of protein kinase CK2. *Mol Cell Biochem*. 2005;274:23–29.
95. Litchfield DW, Bosc DG, Slominski E. The protein kinase from mitotic human cells that phosphorylates Ser-209 on the casein kinase II beta-subunit is p34cdc2. *Biochim Biophys Acta*. 1995;1269:69–78.
96. Zhang C, Vilk G, Canton DA, et al. Phosphorylation regulates the stability of the regulatory CK2beta subunit. *Oncogene*. 2002;21:3754–3764.